PDEng Thesis

DESIGN OF THE PILOT-SCALE VORTEX CHAMBER SPRAY DRYER

Ilias Baiazitov

PROFESSIONAL DOCTORATE IN ENGINEERING
ENERGY AND PROCESS TECHNOLOGY PROGRAMME
CHAIR OF THERMAL ENGINEERING

Examination committee:

Prof.dr.ir. G. Brem (chair and thesis supervisor)
Dr.ir. A.K. Pozarlik (daily supervisor)
Dr.ir. A.P.J. Sweere (company supervisor)
Prof.dr. A.R. Thornton (external examiner)

UNIVERSITY OF TWENTE.

DESIGN OF THE PILOT-SCALE VORTEX CHAMBER SPRAY DRYER

PDEng Thesis

to obtain the degree of
Professional Doctorate in Engineering (PDEng) at the University of Twente,
on the authority of the rector magnificus,
prof. dr. T.T.M. Palstra,
on account of the decision of the graduation committee,
to be defended
on Friday the 15th of June 2018 at 14.00 hours

by

Ilias Baiazitov

born on the 7th of October 1990
in Kostiantynivka, Ukraine

The PDEng Thesis has been approved by:

Thesis Supervisor: prof. dr. ir. G. Brem

Co-supervisor: dr. ir. A.K. Pozarlik

Abstract

The current spray drying technology for milk powder production involves a significant energy input, multiple unit operations (two drying stages and separation) and large installation size. In order to improve the process, the vortex chamber concept has been applied. It is primary characterized by process intensification caused by the presence of high temperatures and velocities of air leading to a considerable reduction of the dryer size. Furthermore, utilization of the vortex flow for both the second drying stage and the product separation, makes it a highly advanced multifunctional system. Finally, a relatively high temperature of exhaust gas allows the potential use of heat regeneration technology that leads to substantial energy saving.

The aim of the PDEng project was up-scaling of the lab-scale vortex chamber spray dryer to a fully operating pilot-scale unit. Computational Fluid Dynamics (CFD) model that was validated for the lab-scale unit, was used for simulating the up-scaled dryer performance. Two design proposals resulted from the undertaken study.

Scaled-up configuration 1 is based on the necessary droplet trajectory length for its complete drying at certain operating conditions. CFD modelling of the obtained design demonstrated the ability to dry the droplets of up to 90 μm at the spray feed of 234 kg/h. The product separation efficiency is equal to 85 % while the energy efficiency is around 6 800 kJ/kg of evaporated water, placing the unit well in the industrial scale operation efficiency of 8 000 kJ/kg in average.

Scaled-up configuration 2 relies on an optimized lab-scale design and is meant for similar capacity and droplets size. However, its performance on a bigger scale became less profitable: obtained separation efficiency of 50 % and energy efficiency of 10 940 kJ/kg are far below the system requirements. This can be explained by non-linearity of occurring phenomena (thus proportional up-scaling of a working solution did not succeed) and a large distance between the drying zone and the vortex flow which negatively influenced separation efficiency. Moreover, usage of the cylindrical inlet for drying of large spray feeds was concluded as not possible due to the droplets contact with the walls. Consequently, feed limitation led to a low energy efficiency.

Subsequently, Configuration 1 was chosen as the optimal one and its economic evaluation was carried out. Besides, the design was analyzed by Technology Readiness Levels (TRL) method and recommendations regarding follow-up steps were given.

Acknowledgments

I would like to express my gratitude towards people and organizations that contributed to both the project development and my personal progress during last two years.

In the first place, I want to acknowledge Rijksdienst voor Ondernemend Nederland (RVO) for the project funding and thus making possible the undertaken research.

The Thermal Engineering group in the University of Twente is an amazing place where I received a high quality guidance from my daily and thesis supervisors dr. Artur Pozarlik and professor Gerrit Brem, while still having a lot of freedom in my own decision making. I want also to thank other group members for their friendliness and many good moments together, namely Alex, Amir, Balan, Citra, Daniel, Harsha, Lucia, Mina, Rafa, Riza and Virginia. Separate thanks are addressed to my project and office mate Umair Jamil Ur Rahman without whom this work would be much less fascinating.

Special acknowledgment is dedicated to the research team from Université Catholique de Louvain - professor Juray De Wilde, Axel de Broqueville and Thomas Tourneur. Thank you for sharing your knowledge throughout our collaboration and your hospitality in Louvain-la-Neuve. Although we disagreed on several aspects, I think that it was beneficial for both sides.

I also would like to thank dr. Anton Sweere (FrieslandCampina) for leading and managing the project as well as Anton Wemmers (ECN) and dr. Albert Poortinga for their input and productive discussions. Finally, I want to acknowledge the Institute for Sustainable Process Technology (ISPT) for their active participation and providing a nice meeting place in Amersfoort.

Table of Contents

Chapter 1

Introduction

1.1 Background

Spray drying technology is a major contributor to the industrial drying field. After the breakthrough as a result of industrial motivated developments in the 1960s *(Masters, 2004)*, the spray drying is utilized now in a wide range of applications and products. For instance, it is adapted in dairy industry for producing of milk powder. Although conventional spray dryers are being successfully operated for that purpose, the need of a more energy efficient system which also incorporates rotating fluidized bed and the function of a separator, led to the concept of the vortex chamber spray dryer.

The vortex chamber concept originates from the research on rotating fluidized beds carried out by *De Wilde and de Broqueville (2008)*. Its further successful application for wet coating of fine particles *(Eliaers et al., 2014)* opened the perspective of an innovative technology for spray drying of milk. Apart from combining three unit operations (1st drying stage, 2nd drying stage and gas/solid separation), the vortex chamber dryer allows significant process intensification *(De Wilde, 2014)* by making use of high-G operation which substantially enhances mass, heat and momentum transfer. Moreover, the energy saving potential of 37 % *(ECN, 2015)* and low construction cost due to a compact size demonstrate that the vortex chamber is a very promising concept for spray drying applications and particularly for milk powder production.

The goal of the present PDEng project is to design a fully operating pilot-scale vortex chamber spray dryer unit, based on the numerical modelling and available knowledge regarding the laboratory scale units. The project is carried out in collaboration with the Institute for Sustainable Process Technology (ISPT), FrieslandCampina, Université Catholique de Louvain (UCL), the Energy Centre of the Netherlands (ECN) and Unilever.

1.2 Stakeholders

There are two stakeholders who represent normal operators i.e. potential users of the design solution. These are FrieslandCampina and Unilever. The aims of FrieslandCampina are related to the implementation of the designed spray dryer in the industry as a very efficient milk powder production unit (in terms of energy consumption and product quality). FrieslandCampina contributes to the project by providing project management, financial support, know-how and data about feeds for drying.

The role of Unilever in the project is to deliver a validation procedure that will involve the supply of a range of different samples to dry and the evaluation of the drying process results. The fact that the stakeholders mentioned above are participating in project management, design,

validation etc., means that they also accomplish the developer function in parallel with end user role.

Developer stakeholders are four other participants: ISPT, UT, UCL and ECN.

ISPT provides research expertise, commercialization expertise, management tools and implementation assistance. Its interest in energy-efficient technologies and fundamental research is the key motivation to participate in this project.

The Thermal Engineering group (TE) at the University of Twente has a considerable experience in the field of atomization, evaporation and droplet formation. The numerical investigation tools used in the related research showed high levels of predictability and are therefore chosen as a design solution platform for the project.

A small-scale lab unit of the vortex chamber spray dryer is designed and operated at UCL. The goal of the team working on that is to investigate energy and process efficiency, product quality and to provide an experimental platform for numerical modelling validation.

ECN's role in the project consists of assistance regarding energy aspects during the design process. It will become very important during the optimization phase of full-scale unit. The overall interest of ECN is related to energy innovation and sustainability.

1.3 Objectives of the design project

The global objective of the project is to accomplish the design of a pilot-scale vortex chamber spray dryer. In order to do that, a reliable numerical model has to be developed. Thus, the 1st design objective can be stated as:

1) Development and validation of the CFD model for multicomponent feed drying.

After the model is proven of having an acceptable accuracy, it will be used as a design tool for dimensioning of the dryer and seeking for an optimal operating conditions window. Therefore, the 2nd design objective is:

2) Dimensioning and optimizing of the vortex chamber spray dryer.

The final step involves a critical consideration of the resulted design. Matching to the requirements, economic evaluation, overall robustness and potential - those are the criteria that have to be kept in mind. So the 3rd design objective comes as:

3) Interpretation and economic analysis of the design solution.

1.4 Design methodology

First, it should be noticed that the project at the current state is between the preliminary and detailed design stage thus this is a suitable period to apply general design process tools. For instance, Design Process Unit (DPU) diagrams are a common tool for introducing and tracking design improvements throughout preliminary and detailed design stages.

The first step in the DPUs' implementation is to categorize all the parameters related to system to be designed. One point of attention here is to indicate a clear difference between design and scenario parameters. These are usually strongly interconnected. On the other hand, only a limited set of scenarios combined with design parameters can lead to the required performance. The overall DPU of the vortex chamber spray dryer is shown in Fig. 1.

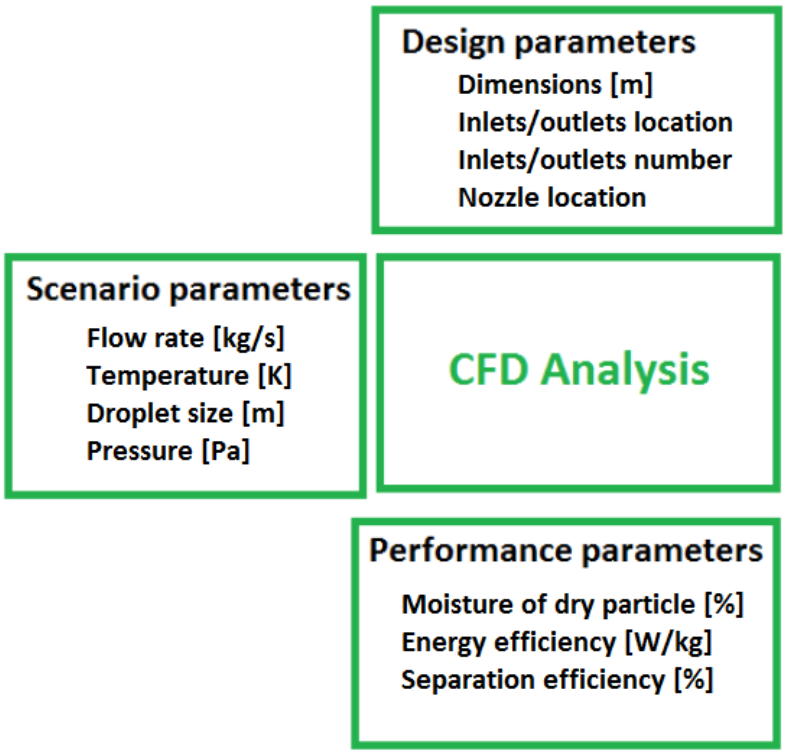

Fig.1 DPU of the vortex chamber spray dryer

The design parameters are mainly related to geometry and space orientation. One of the major challenges is to define an optimal location and the number of inlets and outlets. As illustrated in Fig.2, air is injected from the front section at a certain temperature termed "hot" and through multiple slots in vortex chamber at a "warm" temperature in order to generate vortex flow. The milk spray is simultaneously injected into the vortex chamber from the nozzle. After the droplets are dried to particles, they have to be directed towards the solids outlet(s) while air is leaving through the gas outlet(s). There are various combinations of design parameters which make this a complex research problem.

Scenario parameters include operating conditions of the dryer: flow rate(s), temperature(s), pressure and droplets' size. Even though these are classified as scenario parameters, there is a constant adjustment of these in parallel with the design parameters. For example, droplets size must be reduced if the nozzle is located closer to the outlets in order to afford drying on a shorter trajectory.

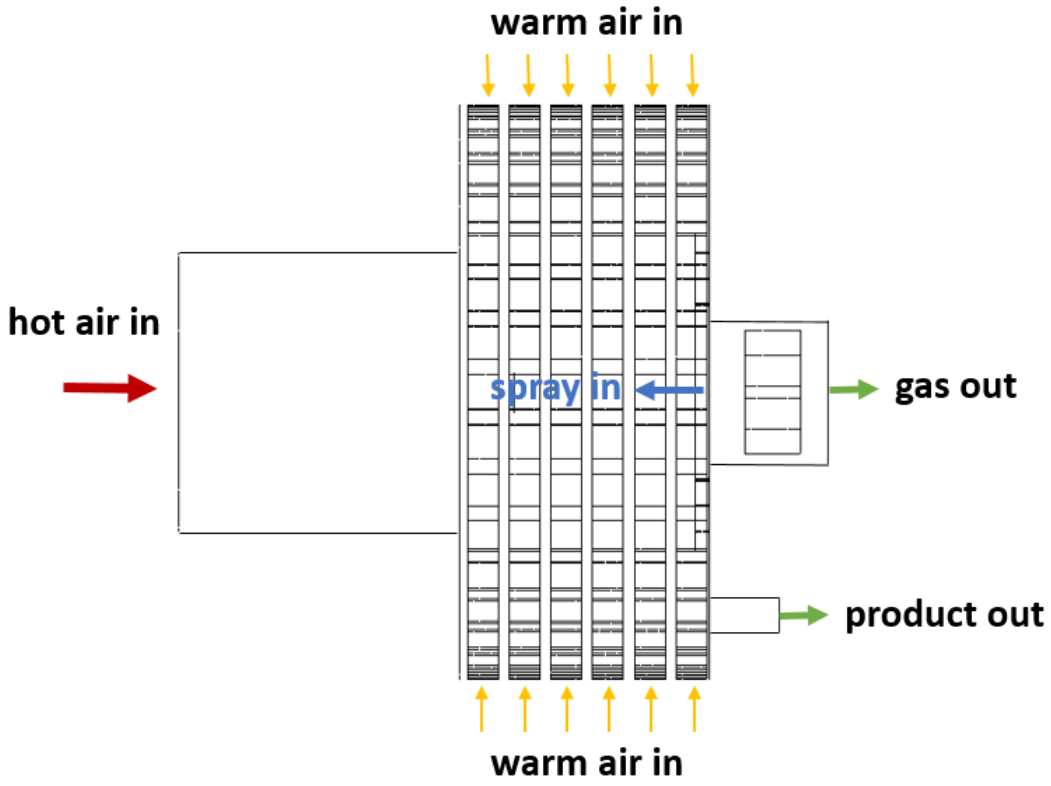

Fig.2 Working principle of the vortex chamber spray dryer

There are three major performance parameters: the moisture of dry particles which reflects the product quality, energy efficiency that takes into account the amount of energy per quantity of product and separation efficiency that indicates the percentage of solids separated from gas. The CFD analysis format is being used here, namely the ANSYS Fluent solver. Various numerical modelling aspects, such as mesh quality or turbulence model, are validated by using experimental data which makes this analysis tool sufficiently reliable for this problem.

Chapter 2

Requirements

2.1 System, process and product requirements

The designed system has to consolidate three unit operations:

1. The 1st drying stage. Injected droplets from the nozzle are going straight into the hot zone where at least 80 % of their moisture must be evaporated. Consequently, droplets get covered by solid crust while remaining moisture keeps evaporating through the pores in the crust. From this moment, high temperature is not necessary anymore and even to be avoided due to the risk of feed burning. Another restriction here is the absence of any particle-wall collision to prevent formation of wall deposits which can be caused by particles still containing water and therefore having favorable properties for stickiness.

2. The 2nd drying stage. After the solid crust formation, remaining moisture has to be removed at a low temperature. Thus, particles must be directed towards rotating fluidized bed which is operated at lower temperature and a higher velocity compared to the hot zone.

3. Powder separation from gas. Besides the 2nd drying stage medium, rotating fluidized bed accomplishes the function of a separator. Dried particles end up by being accumulated in the vortex flow along the chamber walls. Therefore, putting solids outlet(s) at the level of rotating flow will lead to the powder evacuation from the system.

Process requirements can be specified as follows:

1. Energy efficiency. It implies that the energy consumption per kg of evaporated moisture must be at least in the current range of industrial spray dryers. However, the main opportunity for energy saving comes from potential recycling of exhaust air from the gas outlet(s) by heat pump system. In order to make it possible, the exhaust air must be at a relatively high temperature (around 100 °C or higher).

2. Safety. The maximal temperature in the system may not exceed 400 °C due to the risk of powder explosion.

3. Stickiness prevention. The temperature of air in fluidized bed determines the temperature of walls which are in contact with particles. Therefore, the wall temperature must be relatively low (in the range of 100 - 150 °C) while droplets have to be covered by solid crust before hitting the walls in order to minimize the risk of stickiness.

4. Feed temperature. Pre-heating of the sprayed milk is widely used in industry in order to stimulate the drying process. The limit is set at 75 °C due to the milk properties deterioration at a higher temperature.

5. Capacity. The required capacity of a pilot scale unit is around 250 kg/h of feed.

6. Separation efficiency. At least 90 % of powder is expected to be obtained at the solids outlet(s). It is assumed that achieving a higher efficiency would be problematic due to the presence of very small particles that are considered as non-separable within the drying chamber.

The final product properties in the context of drying technology are characterized mainly by its moisture content. A typical amount of moisture in powdered milk obtained from dryer is between 2 and 6.5 % *(Reh et al., 2004)*. However, the CFD model that was used for process simulation takes into account only surface evaporation. This means that estimating of remained inner moisture is beyond the numerical model capacity. Therefore, the criterion of the product quality within the model will be 0 % of remained surface moisture.

2.2 Numerical model requirements

In order to reflect drying process numerically, the CFD model must fulfill the following criteria:

1. Inclusion of all important for the process physical phenomena that are taking place in the vortex chamber spray dryer.
2. Neglecting of secondary factors involved in the process in order to reduce as much as possible the computational time.
3. Accuracy of numerical results that has to be determined by model validation.
4. Good ratio of accuracy vs. computational time (very high accuracy may cause an expensive computational cost).
5. Flexibility for modifying design parameters and quickly obtaining related results.

Chapter 3

Literature review

The aim of this chapter is to present the current state of art of spray drying. Besides the consideration of technological aspects, particular attention is given to the numerical modelling approach. Subsequently, an outline of scale-up methodology and its recent improvements are provided.

3.1 Spray drying technic overview

Spray drying is described by *Nath and Satpathy (1998)* as the transformation of feed from a fluid state into a dried product by spraying the feed into a hot drying medium. The feed can be atomized either by rotating disk or by pressurized nozzle. The droplet temperature while being dried stays low due to the rapid evaporation, thus the spray can contact with a high temperature air without affecting the product quality. Since the spray particles are very small, the resulted drying time is respectively short which allows to process highly heat-sensitive materials such as food or pharmaceutics. Authors propose a systematic approach for investigating the spray drying process which includes five process subdivisions: 1) Atomizer performance studies; 2) Studies on the parametric sensitivity of the spray dryer; 3) Powder property studies; 4) Thermal inactivation studies and 5) Post-drying studies.

Masters (2004) presented an overview of current market-driven spray drying development activities. Among the mentioned tendencies were handling solvent-based liquid formulations, high capacity atomization of abrasive suspension formulations and combining spray drying with other drying technologies (mainly with second drying stage). Motivation behind these improvements is based on several needs such as reducing excessive undesirable product deposit formations, meeting changing market requirements regarding power specifications, reducing the cost of producing a unit weight of dried product and meeting the environmental protection constraints. The reported common industrial problems related to process operation are powder emissions, fire/explosion hazards, contamination source and noise.

Zbiciński and Piątkowski (2004) carried out a series of co-current spray drying tower experiments in order to identify process and atomization parameters of drying and degradation kinetics, spray structure, particle residence time and final product properties. Despite an almost identical particle size distribution in each cross-section of the dryer, negative particle velocities near the axis were observed, which proved the presence of recirculation areas. Analysis of the product properties demonstrated decrease of bulk density due to increase of air temperature. Air-liquid ratio and gas temperature were concluded as the most important factors influencing the drying process.

Another parametric investigation was done by *Birchal et al. (2005)* focusing on the effect of spray dryer operating variables on the milk powder quality. The experiments were performed in a pilot-scale co-current two-stage spray dryer i.e. with a fluidized system connected to the dryer.

The observed particles agglomeration was more likely to occur at higher feed flow rates as well as at higher milk emulsion concentration and consequently resulted in a bigger powder size. Increase of the air inlet temperature led to a faster particle outer crust formation and a higher Hausner number which defines the strength of cohesive force between particles. Several empirical correlations involving final moisture content, powder size distribution, Hausner number etc., were determined and implemented into a mathematical model.

Yazdanpanah and Langrish (2011) studied the performance of a multiple-stage fluidized bed dryer for crystallization and drying of milk powder. The core of this work was to extend a standard conventional spray drying process with the fluidized bed system and to investigate its influence. The results showed a significant improvement in crystallization lactose in skim milk powder within an industrial-feasible process. The post-processing of milk powder in a two- or three-stage fluidized bed dryer led to moisture sorption reduction and 92 % improvement in the degree of amorphicity.

Francia et al. (2015) examined a counter-current swirl spray dryer in order to quantify the influence of wall friction on flow regimes and hence on drying process. Namely, the structure of vortex flow was analyzed at various values of Re, swirl intensity Ω and wall roughness. It was observed that friction on rough walls causes a substantial increase of the turbulence kinetic energy k and the rate of decay of the swirl. The changes of Ω destabilized the flow and led to the formation of recirculation areas. Three different situations were detected depending on the flow regime: central recirculation, no recirculation and annular recirculation. It was concluded that the prediction of flow field in a counter-current swirl dryer is not possible only on the basis of geometry. Moreover, the wall deposits impact both the turbulence values and evolution across the chamber.

The publications discussed in this section indicate the main characteristics of the spray drying technic as follows:

- Spray drying by itself is a single step in product fabrication which also involves the processes of atomization and post-processing;
- Post-processing generally includes second drying stage by means of fluidized bed and separation of particles from air;
- Co- and counter-current spray dryer designs are present on the market. Co-current configuration is more common due to a less complex flow patterns;
- Spray dryers with swirling flow are considerably more challenging for designing;
- Reducing of the energy consumption per unit of product and eliminating undesirable deposits formation (wall stickiness, agglomeration) are the current trends in the context of process improvement.

3.2 Numerical modelling of spray drying

Gretz Zabia (2015) carried out a literature study on CFD modelling for spray drying. Namely, various modelling approaches for simulating continuous and discrete phases as well as turbulence models performance and drying kinetic models were discussed. The overview led to the selection of Shear Stress Transport (SST) model which combines the best features of k-ε and k-ω models for continuous phase modelling.

Fletcher et al. (2006) provided a set of recommendations on how to approach the simulation of spray dryer performance. The necessity to model the process in 3D instead of 2D, as many researchers still do, and to couple continuous and discrete phases was explained and justified. Regarding the turbulence model selection, authors reported a good performance of relatively simple models based on the Reynolds Averaged Navier Stokes (RANS) equations. For instance, the standard k-ε model in case with a fine enough mesh was claimed to be able to resolve the important large scale motions and to model the transport processes at the small scale. The Lagrangian approach for modelling the droplets flow and evaporation was reported as reasonably accurate. However, the presence of solids in particles has to be taken into account in this case. The agglomeration modelling was characterized as very challenging due to the necessity to reformulate well-developed Eulerian models in order to simulate representative droplets for agglomeration. All these recommendations were based on experience from numerical modelling of laboratory-scale, pilot-scale and plant-scale spray dryers. For example, the pilot-scale simulations represented the setup studied experimentally by *Southwell and Langrish (2000)*.

Li and Zbiciński (2006) carried out a sensitivity study on CFD modelling of co-current spray drying process. The resulted list of the most crucial factors includes the gas turbulence model, atomizing air, turbulent particle dispersion, initial atomization parameters and drying kinetics.

Zbiciński and Li (2007) addressed the problem of poor accuracy of CFD predictions for spray drying process in certain range of parameters. Laboratory and pilot plant units have been investigated experimentally and numerically. The obtained data revealed that the current CFD methods provide a good prediction of the continuous phase parameters but the discrete phase is not resolved sufficiently; the smallest error for the discrete phase parameters was on the level of 20 %.

Sagadin and Hribersek (2016) developed a multi stage numerical model of spray drying of zeolite 4A suspension in a counter-current configuration. Its pronounced advantage is in taking into account three stages of drying unlike the common single stage spray drying models. These three stages are: 1) evaporating of surface moisture; 2) removing of moisture from the porous interior of the particle and 3) removing of the remained adsorbed moisture from the zeolite crystals. The latter was modelled by kinetic model based on the thermogravimetry data. The model was validated by comparing the numerical results with the experimental data obtained from the pilot scale spray dryer. The Shear Stress Transport (SST) model was used for turbulence modelling and a two-way coupling between the fluid and the dispersed phase based on Lagrangian approach was utilized. The CFD modelling was used only for simulating the 1st drying stage with sampling

selected particle trajectories and applying them in further calculations for 2nd and 3rd stages. Thus, it could be concluded that CFD modelling is preferable only for the 1st drying stage due to the complexity of simulating evaporation in porous medium.

Ali et al. (2015) studied the detergent slurry spray drying in a counter-current tower. The focus of the work was on particle-wall interaction and related parameters such as restitution coefficient, surface roughness and moisture content. The turbulence of continuous phase was modelled by using Reynolds Stress Model (RSM) and the two-phase coupling was simulated by Eulerian-Lagrangian approach. However, particle-particle interaction and therefore agglomeration and coalescence were not taken into account in order to reduce computational requirements. The results were validated by comparison with experimental outlet values of powder average temperature, moisture content and exhaust air temperature. The main outcome from this study is a developed particle-wall collision model which proves a strong influence of particle-wall interaction on the drying process and the powder characteristics.

Xia et al. (2016) modelled the pre-cooling water spray system in natural draft dry cooling towers. Authors explain their choice of the standard k-ε model by the turbulence sensitivity analysis carried out by *Montazeri et al.(2015)* which reported that none of the studied turbulence models was superior over the others. The numerical results were validated by comparison with the measured outlet air dry bulb temperature and wet bulb temperature. Their good agreement shows the importance to consider the study of *Montazeri et al.* in more details. Apart from k-ε model, four other turbulence models such as the realizable k-ε model, the Renormalization Group k-ε model (RNG k-ε), the standard k-ω model and the Reynolds Stress Model were applied and compared. The average deviation from experimental results was within 10 % for all models thus it was concluded that none of them provides considerably more accurate results than others.

Lal et al. (2017) studied convective scalar transport in a macro porous material for drying applications. The results from utilization of the standard k-ε model showed an excellent agreement with analytical functions even for a high wind velocity of 10 m/s which caused the presence of strong vortices.

Wawrzyniak et al. (2016) investigated moisture evaporation in a dispersed system such as an industrial tower. The Reynolds Stress Model was used for modelling the turbulence within the system. A high amount of instability was reported by authors, for instance, the absence of axial symmetry and oscillations of flow field. However, the experimental measurements of temperature in various cross-sections show a good match with numerical results. Moreover, the agglomeration prediction model, based on the calculated residence time by CFD and the particle size distribution change, was introduced and validated as well.

Although the CFD modelling of agglomeration is considered as difficult to implement, some recent publications present the methods for that. *Jaskulski et al. (2015)* developed their own module for discrete phase simulation which takes into account the hydrodynamic segregation of particles, droplet shrinkage, increases in particle porosity and droplet coalescence. The model correctly predicted the particles diameter growth from 150 to more than 400 μm in a spray tower as well as the final size distribution.

Hou et al. (2012) studied the characteristics of multi-nozzle spray cooling. Although the CFD modelling of two-phase flow and droplets evaporation was accomplished, the emphasis of their work was on the nozzle performance and its influence on the flow behavior. It was observed that the droplet Sauter Mean Diameter (SMD) decreases with the increase of the inlet pressure which increases the mass weighted averaged droplet velocity. The droplet SMD also changes almost linearly proportionally to the variation of mass flux. The resulted spray velocities distribution was not a monotonic function of the nozzle-to-surface distance so the velocity value and the velocity distribution were pointed out as two different targets for optimizing the nozzle-to-surface distance. However, the increase of nozzles number demonstrated a significant improvement in the distribution of droplet size and droplet velocity. The continuous phase was modelled by using the k-ω turbulence model. Its resulted deviation from the experimental measurements stayed below 10 %.

The unsteady RANS and detached eddy simulation (DES) of the multiphase flow in a co-current spray drying were investigated by *Gimbun et al. (2015)*. The purpose of this work was to compare the performance of unsteady turbulence models against the standard steady solvers such as the k-ε model. The DES used in this work is based on the Spallart-Allmaras (SA) turbulence model. The modelled system was identical to the one studied by *Kieviet (1997)* and the numerical results were validated according to his measurements as well. As expected, the unsteady models gave a more accurate prediction of mean velocity, temperature and humidity profiles with error below 5 %. It was also confirmed that anisotropic turbulent flow takes place in the spray dryer based on the velocity component fluctuations and illustrated turbulent structure.

All information about the CFD modelling of spray drying process given above can be summarized into following conclusions:

- 3D modelling is strongly preferred over 2D;
- Two-phase coupling is compulsory for correct process parameters prediction. Though, particle-particle interaction is less significant and may be neglected for reducing computational cost;
- Various turbulence models are being used with a comparative resulting accuracy. Therefore, relatively simple RANS based models can be successfully applied;
- Only the 1st drying stage is worth modelling by means of CFD, otherwise a very expensive computational resources are needed;
- Very sophisticated solvers for modelling agglomeration, wall stickiness and unsteady flow are available and provide a good accuracy for the investigated cases. Obviously, they are more computationally demanding and must be thoroughly evaluated before applying.

3.3 Scale-up methodology

Kerkhof (1994) provided a large theoretical treatment of spray drying process in the context of scaling up on three levels: physical, mathematical and simulation models. It was concluded that

drying process has several complicating factors such as non-linearity of the physical processes, complexity of exchange processes and dependency of dominating phenomena on the drying conditions which may change within the course of drying. In particular, two general rules for scaling up were given. The first one is "*you can never scale-up all phenomena and effects in a similar way*". Thus, the dominating features have to be identified and selected for up-scaling. And the second rule is "*the relative importance of influences may and probably will change with scale*". This means that many parameters may differ on a bigger scale and lead to a dissimilar performance. For instance, drying rate, air temperature and humidity distribution, product particle size and flow and residence time distribution are generally scale-dependent.

Arpagaus and Schwartzbach (2008) reported the procedure applied for scaling up a mini spray dryer to a lab scale unit. The target was to keep the most important process parameters constant and adjust the rest. Among the identified key parameters were the outlet air temperature, the droplet size and the outlet vapor concentration. Therefore, the inlet drying temperature was calculated as a function of water evaporation rate and outlet drying air temperature. The droplet size was adopted through a function of atomization air flow rate for the two-fluid nozzles. The resulted scaled-up configuration demonstrated the capacity to dry up to 10 L/h of feed with the droplet size between 2 and 80 μm against 1 L/h and 2 - 25 μm in the initial design.

Gil et al. (2010) presented scale-up methodology for pharmaceutical spray drying. Their method was divided in two steps: thermodynamic step and atomization and particle formation step. First, the proposed approach requires to keep the same relative concentration of the drying air. The mass and energy balance were therefore used for determining the operating conditions at the commercial scale. In the second step, the two-fluid nozzle used in the lab was replaced by a pressure nozzle producing the droplets of 70-140 μm at 85 bar. The developed commercial installation was operated at 1250 - 1500 kg/h of drying air and 78 kg/h of feed and produced the powder of a similar quality as in the lab scale. The proposed method is recommended to use in case when the product drying behavior is well known and a large experimental data is available.

Thybo et al. (2008) investigated scaling up of the spray drying process from pilot to production scale using an atomized droplet size criterion. Besides the droplet size distribution, the studied parameters were outlet temperature, feed flow rate, solid concentration of feed and open/closed cycle. The carried out up-scaling based only on matching atomizer droplet size distributions was not successful due to the necessity to take into account more parameters such as residence time or droplet temperature. However, the operating conditions could be adapted by trial-and-error method and resulted powder characteristics did not differ from those obtained out of the pilot-scale dryer.

It can be concluded that scale-up procedure is a challenging engineering task. The following considerations must be taken into account while undertaking the scaling up:

- It is impossible to project efficiently all phenomena on a bigger scale;
- Spray drying process is very dependent on the nozzle performance at any scale;
- There are no universal up-scaling rules, each case must be treated individually.

Chapter 4

CFD model description

In this chapter, a detailed description of the CFD model is provided. Dimensions, grid quality, numerical methods and boundary conditions – those are the key aspects to be discussed together with the assumptions that led to final selection.

Computational Fluid Dynamics is a numerical method for solving Navier-Stokes equations that do not have a general analytical solution. Thus, the iterative approximation is used for resolving the equations over a divided in multiple grid cells domain. The solution accuracy depends on many factors: grid size, discretization scheme, turbulence model, assumptions regarding boundary conditions, etc. and it is usually verified by comparing CFD results against experimental data. Therefore, it is very important to specify the appropriate input parameters in order to obtain a rigorous solution.

4.1 Geometry

4.1.1 Scaled-up configuration 1

Apart from affording a bigger production capacity, the aim behind up-scaling is also to achieve the drying performance which is problematic to arrange on a smaller scale. The major issue, reported from experiments on the laboratory scale unit of the vortex chamber spray dryer, was the large deposits on interior walls. This indicates that particles were not dried enough at the moment when they were impinging the walls. An explanation of incomplete drying can be related to a short residence time in the hot zone and/or an insufficient temperature. Moreover, small dryer size and even smaller area of the hot zone with presence of the air velocities ranging from 10 to 15 m/s are likely to be the source of the encountered problem. Therefore, it is necessary to determine the exact time and trajectory length of sufficiently dried particles for designing a chamber that would be large enough to avoid the stickiness problem.

In order to investigate evaporation process of single particles, CFD modelling of water droplets drying in a cylindrical tube was carried out. The simulated system and its boundary conditions are shown in Fig.3. The process parameters were chosen such as those that take place in the designed spray dryer. Thus, the air velocity was set at 10 m/s and the particles feed temperature at 75 °C. The initial mass fraction of water was set at 0.6. Similar conditions were used later in the scaled-up configurations. The flow was modelled by using RANS k-ε model with 2-way gas/particle coupling which selection is explained in Chapter 3.2.

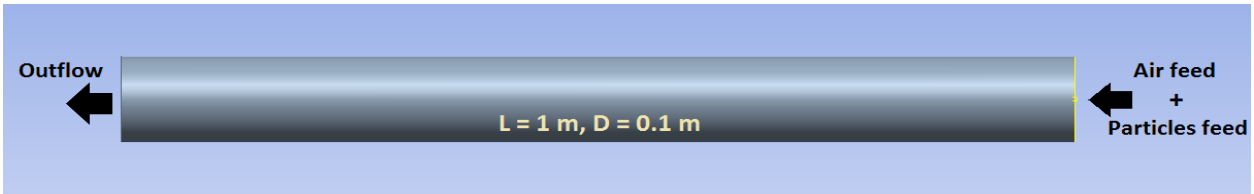

Fig.3 Test tube for evaporation modelling

The first simulation was carried out with the air temperature of 350 °C and the particles size of 63 μm injected at the velocity of 54.7 m/s which correspond to the expected SMD and feed velocity from the nozzle applied in the lab-scale unit. It can be seen in Fig.4 that complete water evaporation occurs in the middle of the tube i.e. after passing the distance of 0.5 m that takes 0.03 s. The obtained results suggest that the minimal particle trajectory length before it hits the wall must be equal to 0.5 m. Since the temperature of 350 °C is not the highest one allowed in the process, another test was made with the temperature of 390 °C in order to check the influence of such a temperature on drying time. It resulted that complete water evaporation, observed in Fig.4 occurs at 0.025 s after injection. The obtained difference of 5 ms compared to the case with 350 °C does not seem very important but it should be noticed that the presented tube tests were performed with a small feed flow rate which did not lead to significant temperature drop in the tube. However, extensive and rapid evaporation in a compact spray dryer will cause a considerable temperature drop and particles would need a larger drying time. Therefore, it is substantial to assure the initial heat input at an as high as possible temperature. According to the safety requirements from Chapter 3, the temperature of 390 °C is almost at the allowed limit. Thus, the preliminarily chosen temperature of air in the hot zone is 390 °C.

Due to the prescribed SMD equal to 63 μm, the particles size distribution will include the sizes both below and above the SMD. It implies that the spray dryer volume must be large enough for drying the particles which are significantly bigger than their SMD. Moreover, potential droplets agglomeration can also lead to a bigger particle size that has to be dried. Consequently, another test tube simulation was done for the particle size of 100 μm. It can be seen in Fig.6 that the distance of 1 m is sufficient just for reducing the moisture content to 0.15.

The test tube simulation results presented above were used as an indicator for dimensioning the spray drying chamber. Thus, by assuming the aimed particle trajectory length of 1 m (for the biggest particles) and counter-current configuration, the resulted chamber length must be at least equal to 0.5 m. Since the nozzle tip cannot be located at the back wall level, some additional space is necessary for that. Consequently, the final length of the chamber was set at 0.525 m. The chamber diameter has to be big enough for ensuring the presence of a large hot zone in the middle of the chamber i.e. the influence of the cold air injected through the slots on the drying temperature must be minimized. Moreover, the hot air inlet size should be also large enough for assuring such conditions. It is assumed that the major part of drying occurs during the axial movement of particles forth and back, so the radial dimension of the hot zone (determined by hot air inlet) may be less than the chamber length. Thus, the hot air inlet was set at 0.3 m.

Finally, the chamber diameter was determined by ratio ≈ 2 to the hot air inlet for preventing possible backflow of warm air to the cylinder and resulted in size of 0.618 m.

The slot dimensions within the 6 wheels configuration were adapted for having a uniform distribution of the vortex flow over the chamber. The solids outlet was located at the level of rotating flow for catching the dried particles from their biggest concentration area. Whereas, the gas outlets were put in the center of chamber behind the nozzle i.e. in the area where no particles are expected to circulate. The outlets dimensions are arbitrary and have to be optimized based on the final design operating conditions. A schematic drawing with the major design dimensions is shown in Fig.7.

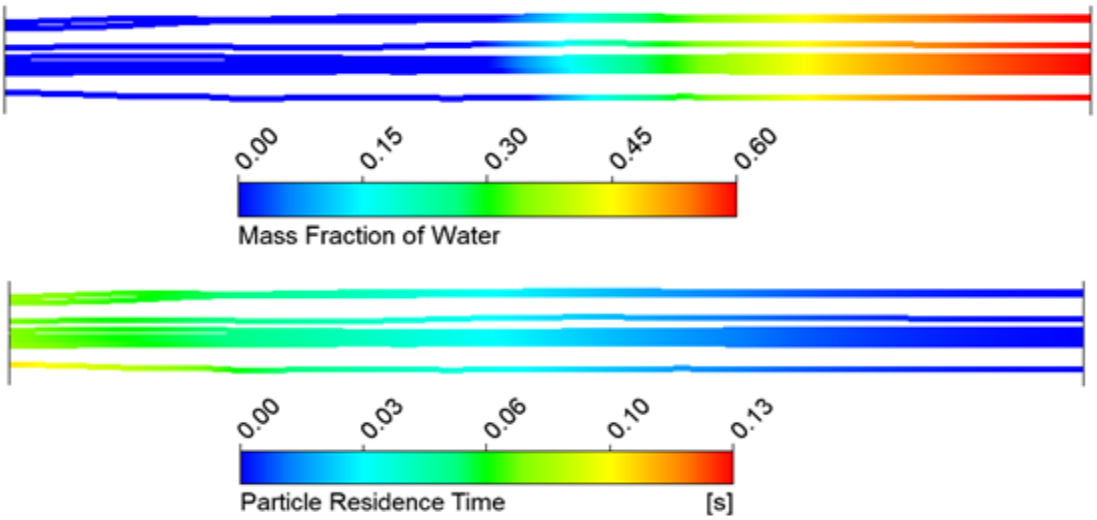

Fig.4 Evaporation of particles of 63 μm at 350 °C

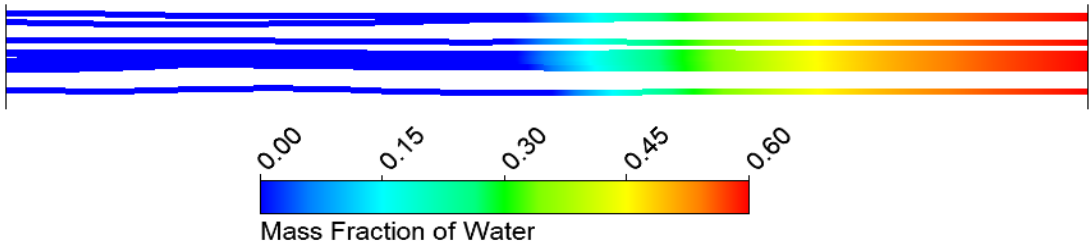

Fig.5 Evaporation of particles of 63 μm at 390 °C

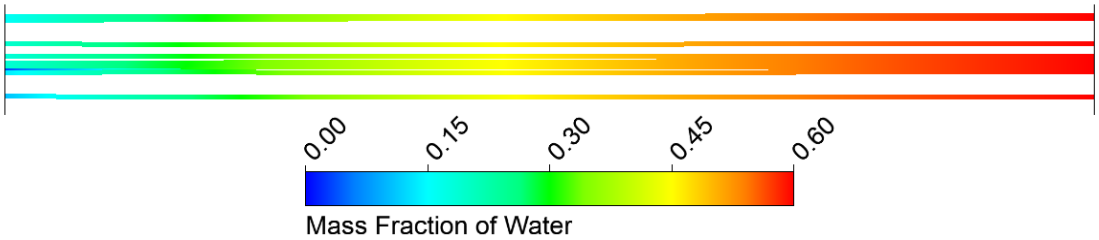

Fig.6 Evaporation of particles of 100 μm at 390 °C

4.1.2 Scaled-up configuration 2

Unlike the previous design, the second scaled-up configuration was not developed analytically. It is based instead on an existing laboratory scale unit for which an optimal operational window has been adapted by parametric study through a validated CFD model. However, its volume was set equal to the volume of Scaled-up configuration 1 in order to compare the performance of two different designs which have comparative dimensions. Hence, the initial laboratory configuration with the volume of 0.03 m^3 was up-scaled to 0.18 m^3 which stays in the same range as the Configuration 1 volume of 0.17 m^3. To do that, each dimension (x, y and z) was increased by factor 1.8.. The sketch of the resulted design is shown in Fig.8.

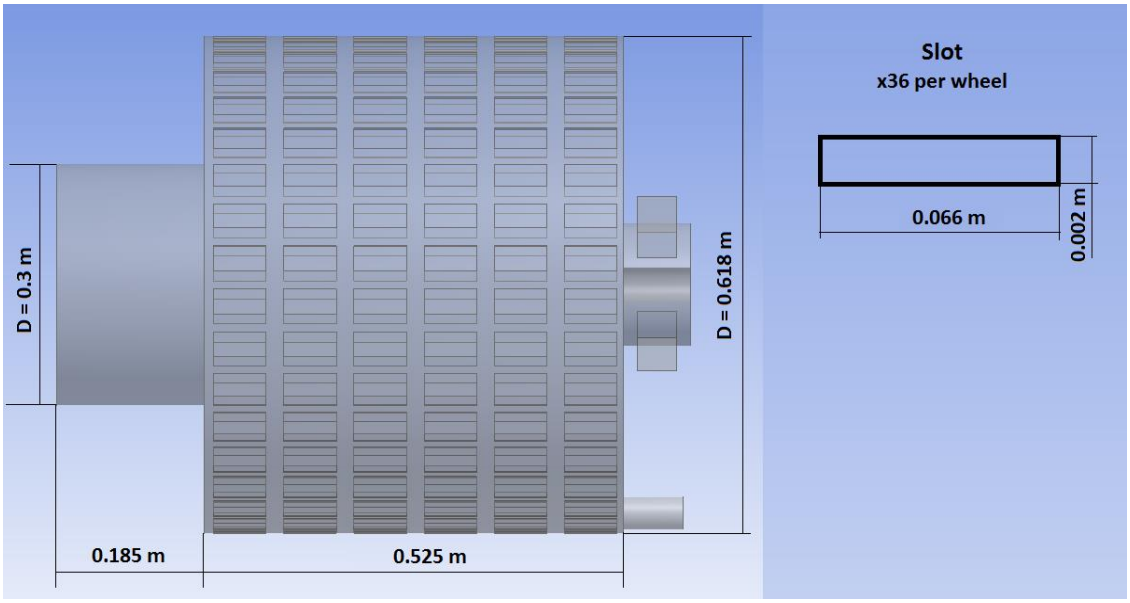

Fig.7 Sketch of Scaled-up configuration 1

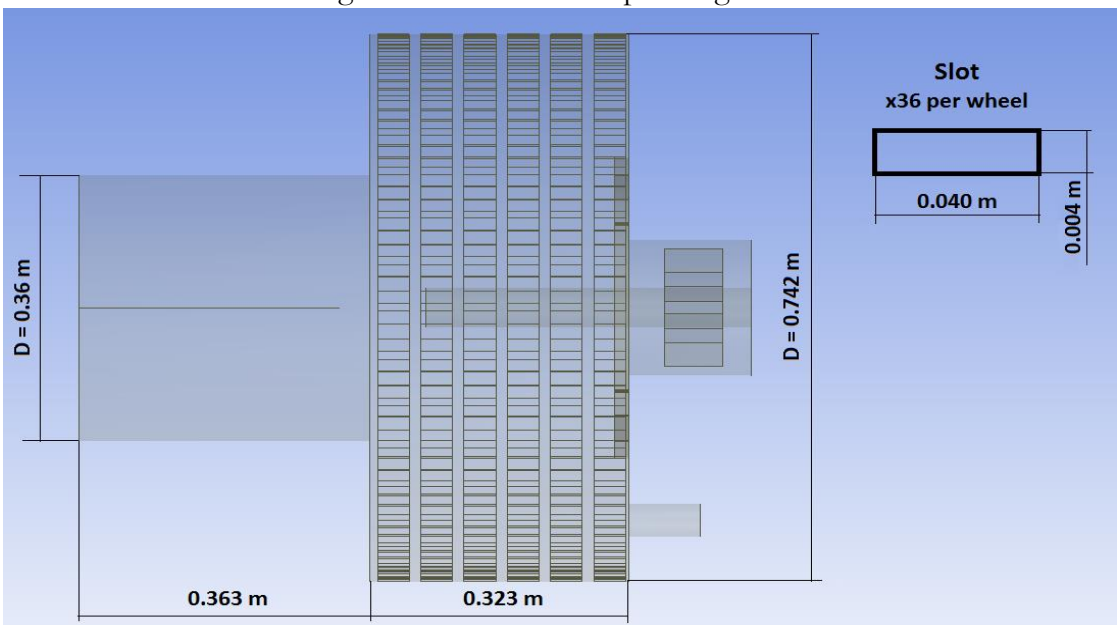

Fig.8 Sketch of Scaled-up configuration 2

It can be summarized that two configurations presented above have similar volumes but significantly different proportions and working principles. For instance, the cylinder in Configuration 2 serves as an extension of the chamber and it is meant for drying particles, while the cylinder in Configuration 1 is designed only as an inlet and no particles are expected in there. For this reason, the chamber in Configuration 1 combines both drying and separation functions while in Configuration 2 it is used only for particles separation.

4.2 Grid

The grid aspects is a critical parameter in numerical modelling. In order to obtain accurate simulation results, the grid quality must be such that any further mesh refinement would not change the solution outcome, i.e. the results have to be grid independent. Therefore, the grid independency tests were carried out for each design. To accurately capture the investigated phenomena, a uniform grid size was used.

4.2.1 Scaled-up configuration 1

The grid independency tests were performed by simulating the air flow at the same conditions but with different number of mesh elements. Three cases have been investigated: 2.9 million, 5.9 million and 8.9 million elements in each.

An in depth examination of temperature profiles was done at various locations as shown in Fig.9. Although the obtained patterns are very similar (see Fig.10), there are small differences in profiles for Line 2 and for the top part of Line 3. Both of these regions are characterized by intensive mixing of cold and hot air which means that those zones need a finer grid. However, the coarsest grid demonstrates the same pattern and the maximal difference between results is equal to 5 K. Therefore, it can be considered that the 2.9 M mesh is a suitable one for further simulations. Though, the difference in temperature must be kept in mind during the analysis of future results.

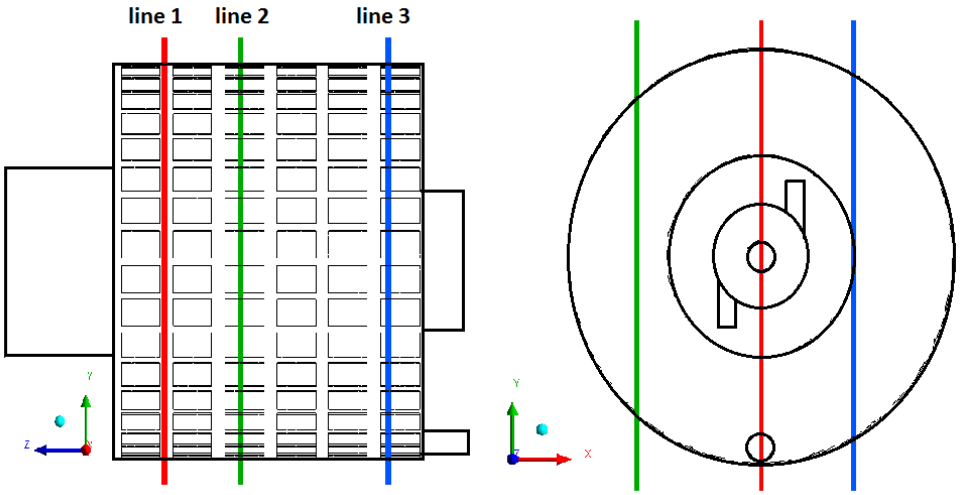

Fig. 9 Characteristic lines location

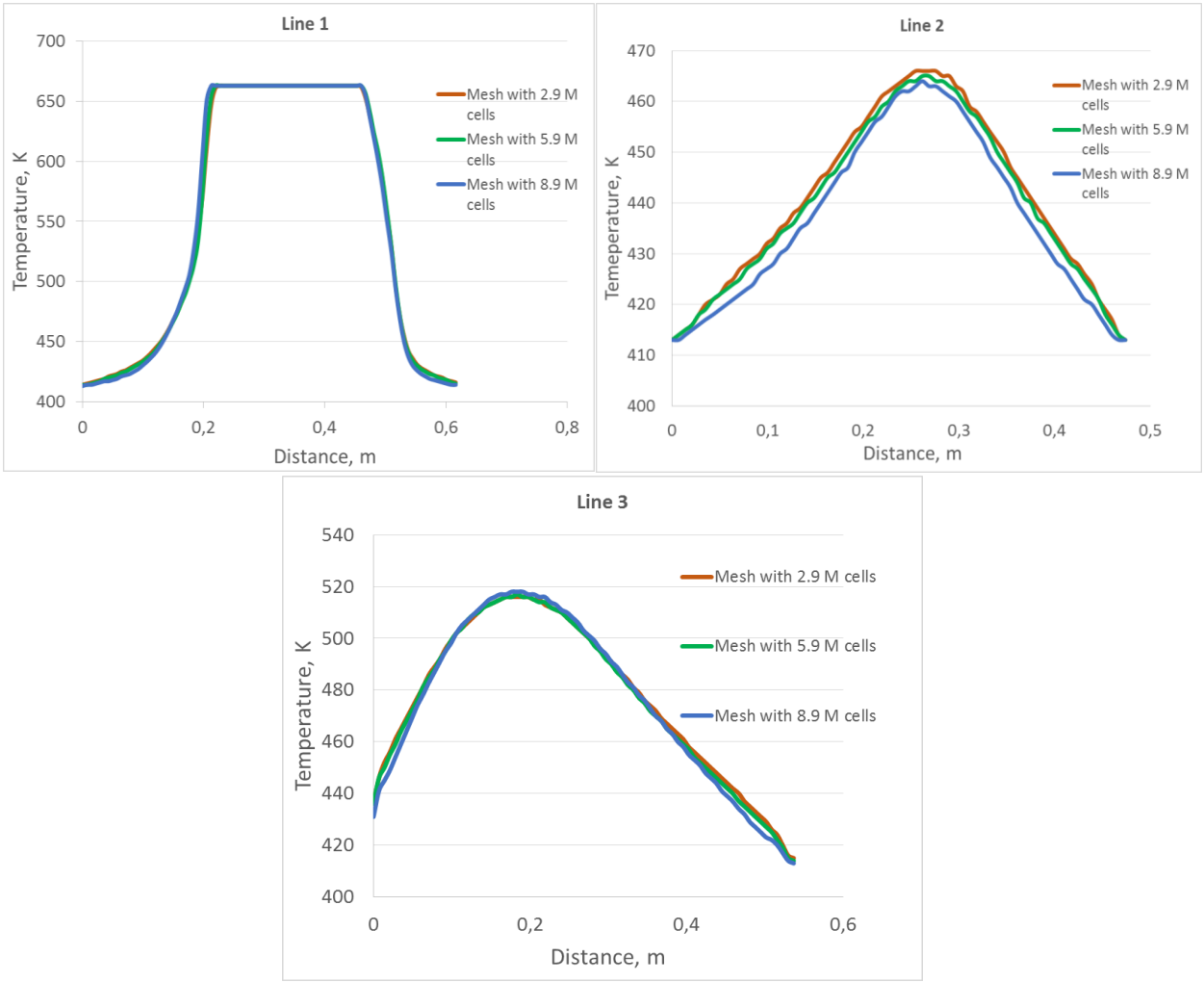

Fig.10 Temperature profiles for investigated grids of various locations

4.2.2 Scaled-up configuration 2

By the same manner as for Configuration 1, the grid independency tests were carried out for Configuration 2. The grid size of 3 million elements was selected for further modelling. The detailed mesh validation procedure is given in Appendix 1.

4.3 Turbulence model selection

Application of various turbulence models was overviewed in Chapter 3. Although most of the studied publications claimed a sufficiently accurate performance of simple RANS models such as the standard k-ε model, it is preferable to test them in more details. Therefore, several different turbulence models were applied to one of the previous laboratory-scale designs of the vortex chamber spray dryer (*Gretz Zabia, 2015*). That particular configuration (see Fig.11) was chosen due to available experimental measurements.

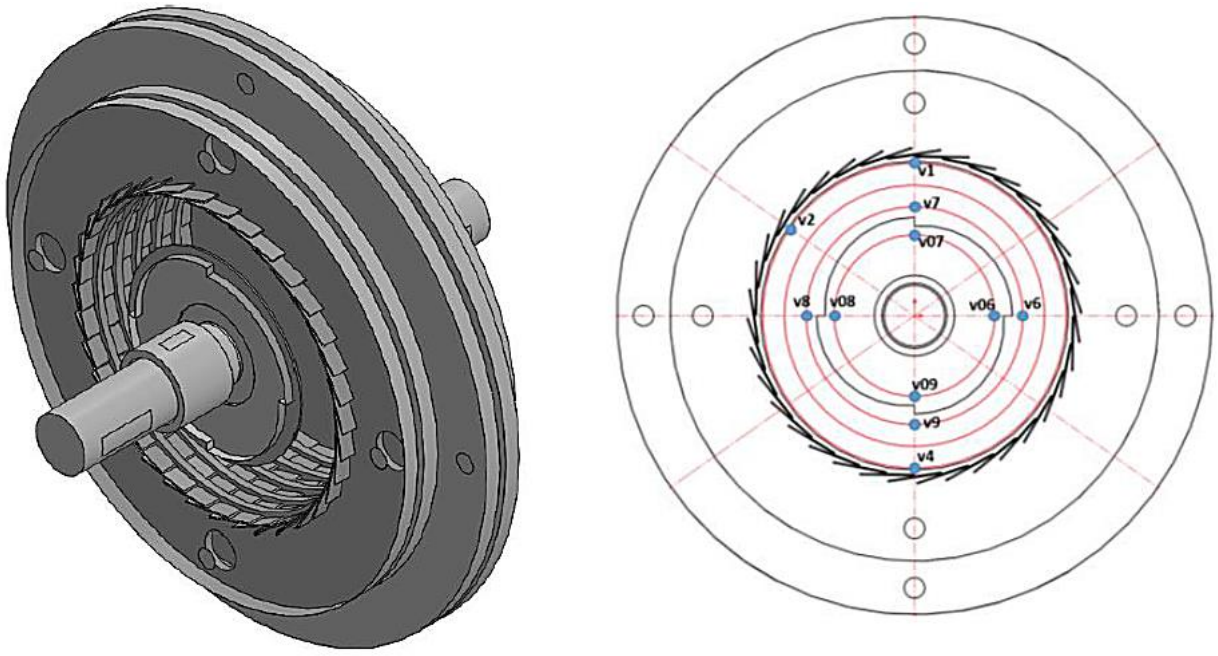

Fig.11 Lab-scale vortex chamber dryer (left) with location of the measurement points (right), *(Gretz Zabia, 2015)*

Thus, 3 turbulence models were tested and compared:

- Standard RANS k-ε model
- RANS Shear Stress Transport (SST) turbulence model
- Large Eddy Simulation (LES)

Figure 12 presents the obtained numerical results as well as the experimental values at various locations in the vortex chamber. The observed patterns are similar for each turbulence model.

However, the SST model showed the best level of accuracy while the LES model results were the least accurate. However, the LES model is supposed to be more realistic due to the non - steady state (transient) solver and large scale eddies resolving. The reason of its reduced performance can be an insufficiently small grid cells used in the simulation (the LES model generally requires a fine mesh). The used grid contains 6 million elements which is considered as the limit due to a very expensive computational time even for steady-state models. It has to be noted that in the simulations the heat losses via the walls were neglected. Although the SST model shows a better prediction than other models, it is considerably more computationally demanding. Therefore, the RANS k-ε model as computationally the cheapest and following the same trend as other investigated models, it is chosen for further application.

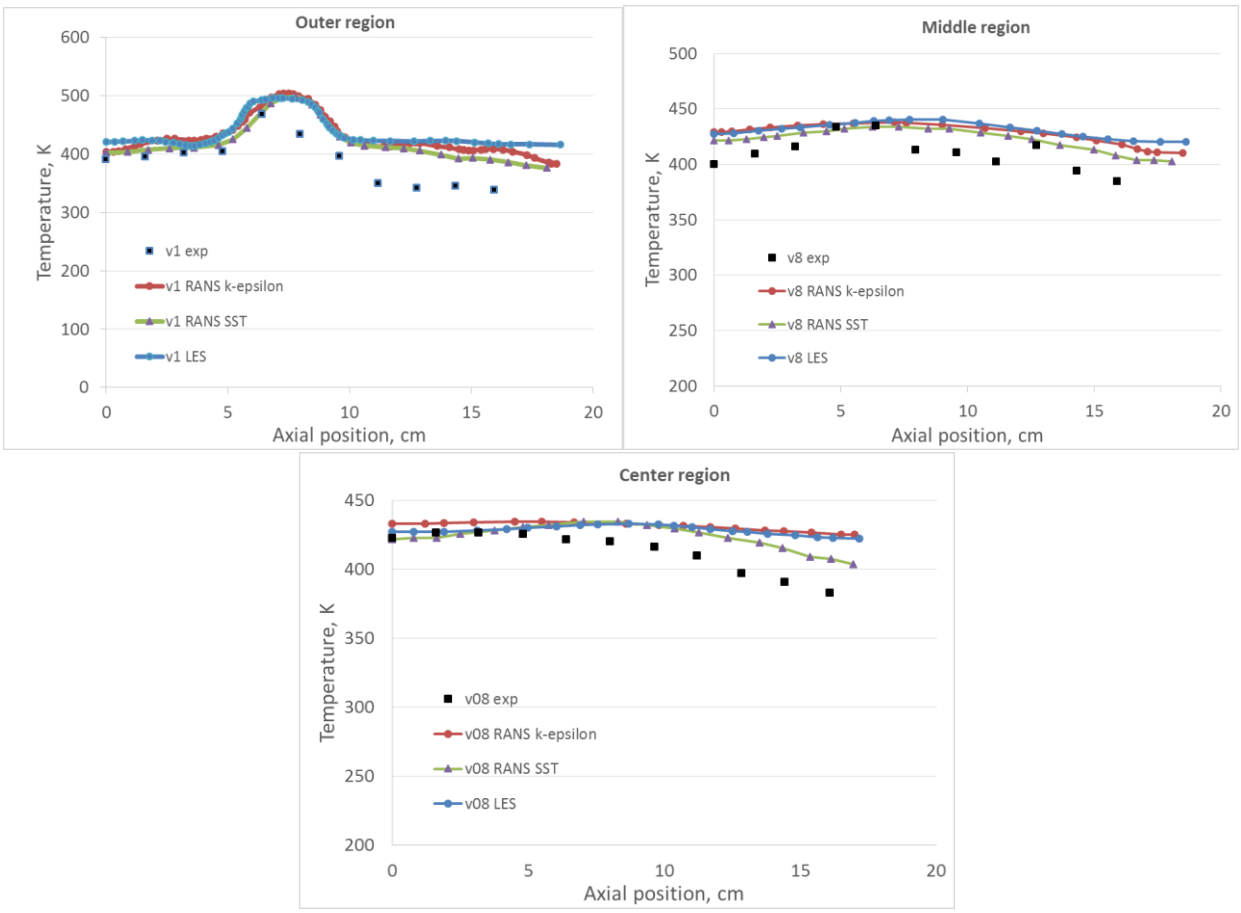

Fig.12 Results comparison from various turbulence models to experimental measurements

4.4 Multi-phase model

The multi-phase simulations were performed through the discrete phase model i.e. the particles or droplets flow model. The model computes particles trajectories in Lagrangian frame and couples heat, mass and momentum equations with the gas phase that is in Eulerian frame. Two-Way Turbulence Coupling (*ANSYS FLUENT 12.0 User's Guide, 2009*) was included for

calculating the effect of particles on gas turbulent quantities which are likely to change due to interaction with spray particles. Furthermore, Temperature Dependent Latent Heat ((*ANSYS FLUENT 12.0 User's Guide, 2009*) for including the droplet temperature effects on the latent heat was applied.

The milk drying process is difficult to model due to physico-chemical properties of milk and porosity of the droplets core. Therefore, application of a multi-component model is a common way to represent it numerically *(Robjer Gullman, 2010)*. This implies that the injected particles consist of a solid core and water around it as shown in Fig.13. Hence, only surface evaporation is taken into account and after all moisture is removed, the remained solid core represents powder particle. In order to implement this model, it is important to specify the right initial content of moisture and the components densities. The amount of moisture in the feed to be removed by spray drying process is equal to 60 %, therefore the initial water content was set at that value. However, the density of injected milk is at 1000 - 1200 kg/m^3 depending on the amount of fats and proteins, while the milk powder particle density is around 1200 kg/m^3 (*Sharma et al., 2012*). Consequently, the overall particle density was adapted to 1185 kg/m^3 by combining the water density of 975 kg/m^3 at 75 °C and the solid core density set to 1500 kg/m^3.

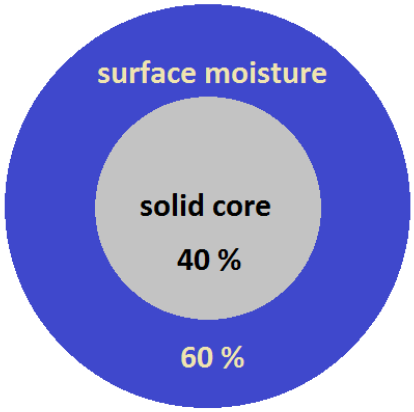

Fig.13 Multi-component particle model

It is also crucial to prescribe correctly the spray injection parameters such as SMD and injection velocity. These parameters were calculated through experimentally determined relations, see Eq. (1) and (2) by *Klaassen (2016)*:

$$SMD = 3189 \times d_e^{0.2267} \times \left(\frac{\Delta P^{\frac{3}{2}} \times FN \times \rho^{\frac{1}{2}}}{\sigma \times \mu} \right)^{-0.05077 \times FN^{-0.06122}} \quad (1)$$

$$V_{inj} = \sqrt{\frac{2 \times P_{at}}{\rho}} \quad (2)$$

where d_e is the nozzle diameter, P_{at} is atomization pressure, ΔP is the difference between atomization and atmospheric pressures, ρ is the liquid density, σ is the liquid surface tension, μ is the liquid dynamic viscosity and FN is the flow number which is described by Eq. (3):

$$FN = \frac{Q_{liq}}{\sqrt{\Delta P \times \rho}} \tag{3}$$

where Q_{liq} is the liquid volumetric flow rate.

As it was explained in Chapter 3, the particle-particle interaction is extremely costly for computing and therefore was neglected in the model. However, particle-wall interaction is taken into account. The determining parameter for it is the restitution coefficient which was fixed to 0.2, based on work of *Gretz Zabia (2015).*

4.5 Boundary conditions

The cylindrical hot air inlet and rectangular cold air inlets (slots) around the wheels are presented in Fig.14. The air injection was modelled by imposing mass flow rates through the inlets. Therefore, the obtained velocities are determined by the ratio between flow rates and inlet surface areas. In view of the identical size of cold air inlets and their grouped selection, an imposed flow rate is evenly divided and thus leads to uniform momentum distribution over each wheel. Thus, it is assumed that the air is uniformly distributed over the slots. In the experimental setup, each wheel or a set of wheels has a jacket around where the air is injected through 4 to 8 inlets. Consequently, velocities at the slots of the same wheel may vary depending on the jacket configuration. It is assumed that this difference between numerical and experimental geometry is negligible for flow pattern inside the vortex chamber spray dryer.

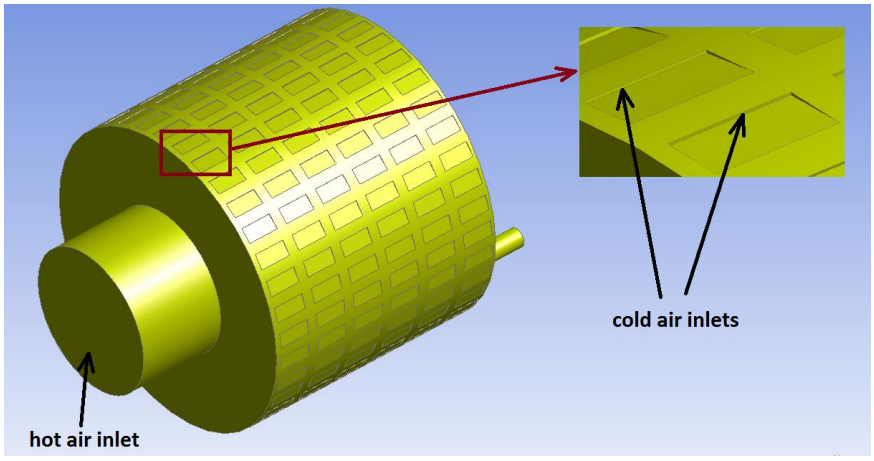

Fig.14 Inlets location of Configuration 1

There are two types of outlets: for gas and for solids (powder), see Fig.15. Both of them were modelled as pressure outlets. The pressure values were taken from experimental operating conditions: 100 mbar at the gas outlets and 60 mbar at the solids outlet.

The process was modelled as adiabatic i.e. no heat losses via the walls were taken into account. The wall shear condition was set as the no-slip due to its interaction with air which is a viscous fluid.

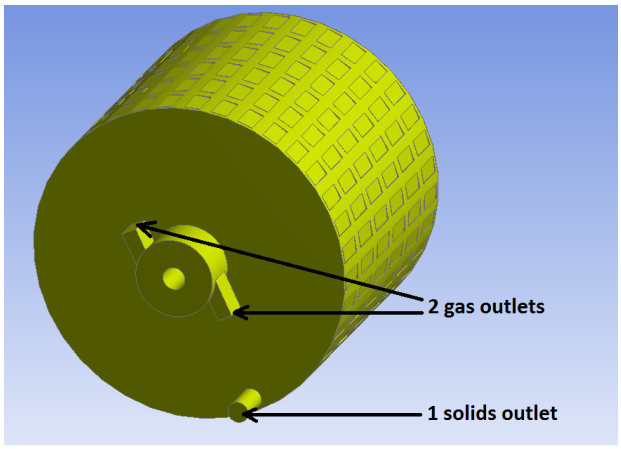

Fig.15 Outlets location of Configuration 1

Chapter 5

Design of Configuration 1 based on the particle drying time

5.1 Parametric analysis

The aim of parametric investigation is to identify and optimize of the key factors influencing the drying process. Therefore, each following subchapter includes analysis of a particular parameter effects and the undertaken steps for achieving a desired performance of the vortex chamber dryer.

5.1.1 Influence of flow rates

There are two different air inputs to the system: hot air through the cylinder and cold air through the wheels slots. It is important to find out an optimal ratio between them that would satisfy the following criteria:

- hot air flow ($\dot{M}_{hot}$) rate is big enough to generate a large hot zone in the middle of the chamber in order to maximize the particles residence time in the hot medium and thus complete their drying;
- cold air flow rate ($\dot{M}_{cold}$) is large enough to create a strong vortex flow which is meant to entrain the particles from the hot zone, and direct them to solid outlet while being still separated from the hot air flow.

Thus, three different cases are taken into consideration: $\dot{M}_{hot} = \dot{M}_{cold}, \dot{M}_{hot} > \dot{M}_{cold}$ and $\dot{M}_{hot} < \dot{M}_{cold}$ respectively. While increasing one flow rate relatively to another, the used ratio $\frac{\dot{M}_{hot}}{\dot{M}_{cold}}$ is in the range of 0.9 - 1.1. This is done for constant T_{hot} and T_{cold}.

Although the temperature distribution change for all investigated cases is minor, the flow rates variation causes the velocities change which has a significant impact on the particles trajectories and thus on the whole drying and separation process. Therefore, the same operating conditions were examined together with the spray injection in order to check the flow rates impact on drying and separation. Fig.16 shows the influence of flow rates ratios on the drying of particles from 30 to 90 μm (Rosin-Rammler distribution) for different $\frac{\dot{M}_{hot}}{\dot{M}_{cold}}$ ratios. It can be seen that the presence of a bigger amount of hot air is essential for completing drying in the hot zone before the particles approach the walls. As it is observed for $\dot{M}_{hot} = \dot{M}_{cold}$ and $\dot{M}_{hot} < \dot{M}_{cold}$, many particles still have a large mass fraction of water (0.2 - 0.35) when they touch the back side of the chamber, while much less particles with a lower water fraction (0 - 0.15) end up at the same location for $\dot{M}_{hot} > \dot{M}_{cold}$. The particles deflection towards the gas outlets is present in all cases

but for the $\dot{M}_{hot} > \dot{M}_{cold}$ case is the highest (54 % vs. 47 % for the $\dot{M}_{hot} = \dot{M}_{cold}$ case). This means that a further increase of the hot air flow rate will lead to a lower separation efficiency and most probably to lower energy efficiency due to a larger energy input. Therefore, the ratio of 1.1 between the hot and cold air flow rates is chosen as a compromise in terms of drying and separation performance.

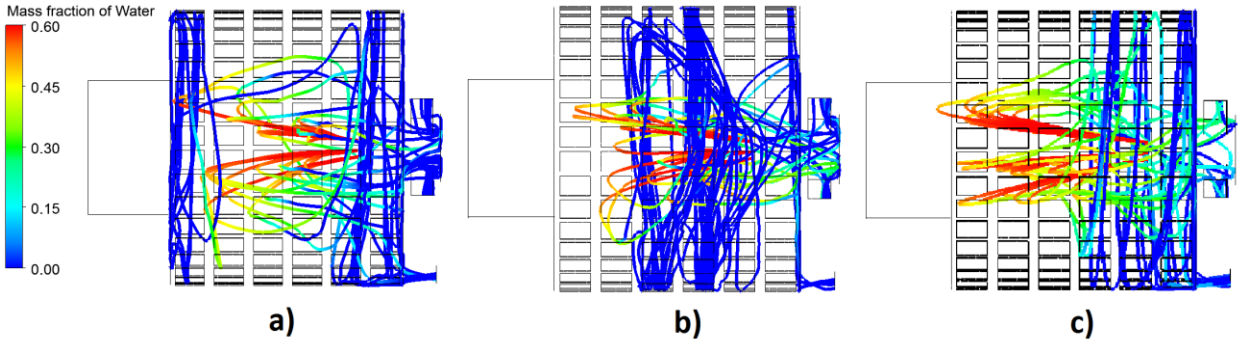

Fig.16 Evaporation of particles at different flow rates ratios: a) $\dot{M}_{hot} > \dot{M}_{cold}$, b) $\dot{M}_{hot} = \dot{M}_{cold}$, c) $\dot{M}_{hot} < \dot{M}_{cold}$

5.1.2 Influence of the nozzle location

First of all, it should be noted that while prescribing the nozzle location in the CFD model, the injected particles have immediately the imposed size distribution at that point. In reality, a certain size distribution is the one which takes place after the primary breakup of the jet. Therefore, the distance from the nozzle tip until the primary breakup zone which is around few millimeters has to be taken into account while implementing the presented recommendations. Secondly, the goal of the nozzle location investigation is to minimize the influence of the gas outlets on the droplets pathways. In other words, the nozzle must be distant enough from the outlets but not too deep in the chamber in order to use efficiently the hot flow and avoid solid losses via gas outlets.

The tests were performed on the configuration with the solid outlet located at the front plate which is discussed in Chapter 5.1.5. Injection of particles having the uniform size distribution of 50 µm was modelled at three different locations shown in Fig.17. The indicator of performance evaluation was the amount of particles (in mass percentage) escaped through the gas outlets. The obtained amounts are as follows: 30 % at location 1, 10 % at location 2 and 0.2 % at location 3. It follows that putting the nozzle close to the back plate results in a big amount of particles deflected backwards. Although the nozzle position 3 demonstrates the best results, it is too close to the cylinder and thus the particles residence time will not be sufficiently long for complete drying of droplets as was discussed in Chapter 4.1.1. Therefore, the location 2 is chosen as the most promising for further tests.

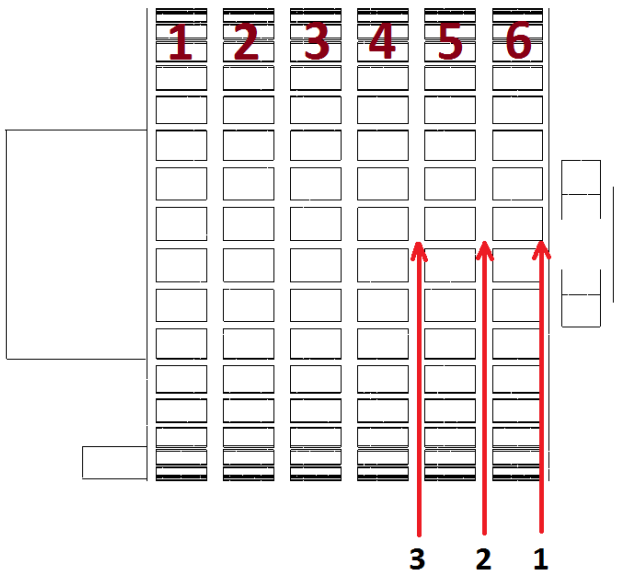

Fig.17 Tested nozzle locations

5.1.3 Influence of G-force

Separation process in the vortex chamber is driven by G-force that is calculated as follows:

$$GF = \frac{V_t^2}{rg} \tag{4}$$

where V_t is the tangential velocity of air, r is the radius of the chamber and g is the acceleration constant equal to 9.81 m/s^2.

The only variable in the formula (4) is the velocity which is defined by the slot surface area and the imposed flow rate. Since the slot size is constant, the cold air flow rate is the single adjustable parameter. However, it is possible to impose different flow rates at each wheel in order to have variable G-force across the chamber. The simulations which results are represented in Fig.16 had a uniform flow rate distribution of 0.45 kg/s that results into the tangential velocity of 18 m/s. Its substitution to expression (4) leads to maximal GF = 107 g. Since this was not strong enough for efficient separation, a higher values of G-force have been considered and studied.

First, a local increase of G-force at the wheels 5 and 6 was introduced (wheels numbers are given in Fig.17). A series of tests with gradual increase of cold air flow rate at these two wheels was carried out. Its summary is provided in Table 1. It can be seen that the local increase of G-force at two wheels does not lead to significant separation improvement. Therefore, the G-force was increased across all the wheels as specified in Table 2. A relatively good improvement is observed only with GF = 428 g that requires a twice bigger amount of cold air. Such an amount of cold air makes the hot zone shrink which substantially reduces the drying potential. Even with such a high value of G-force the resulted separation efficiency is only at 70 % which is significantly below the required one of 90 %.

It can be thus concluded that the increase of G-force requires a large amount of cold air which is not acceptable as was concluded in Chapter 5.1.1. Therefore, the key to efficient separation should be looked elsewhere, for instance, by changing the number and location of solids outlets which is discussed in Chapter 5.1.5.

Table 1 Local G-force increase tests at the wheels 5 and 6

Relative flow rate increase	G-force	Separation efficiency
+ 10 %	129 g	47 %
+ 20 %	154 g	48 %
+ 30 %	181 g	47 %
+ 50 %	241 g	51 %

Table 2 Uniform G-force increase tests (all wheels)

Relative flow rate increase	G-force	Separation efficiency
+ 50 %	241 g	55 %
+ 100 %	428 g	70 %

5.1.4 Influence of the nozzle parameters

According to the literature study given in Chapter 3, selection of nozzle parameters is the crucial step in the spray dryer design procedure. In fact, one of the common approaches is to select a certain nozzle and design the spray dryer for the particular spray conditions. A possible drawback of such an approach is a mediocre robustness. Hence, the undertaken design study involved the tests of various spray parameters in order to determine their influence on the process and the operational window regarding the nozzle specifications.

There are three major spray parameters that significantly influence the interaction between drying air and particles: spraying angle, injection velocity and particles size. The feed rate is equally important but it is considered separately in Chapter 5.1.6 in the context of the system capacity.

Since the hot zone is located in the middle of the chamber, it is necessary to spray particles at a sharp angle in order to maximize their residence time over there. Otherwise, particles will be quickly picked up by the vortex flow far before the drying is complete. For that reason, various small values of spraying angle α have been tested. It follows from Fig.18 that the angles of 40 and 30 degrees are too large so the spray "opens" too fast and the particles hit the walls while being still wet. Thus, the angle of 20 ° shows the best performance while the value of 10 ° leads to significant deflection backwards that can be explained by the highest velocity in the center of the hot air flow to which the particles are directed with such a small spray angle.

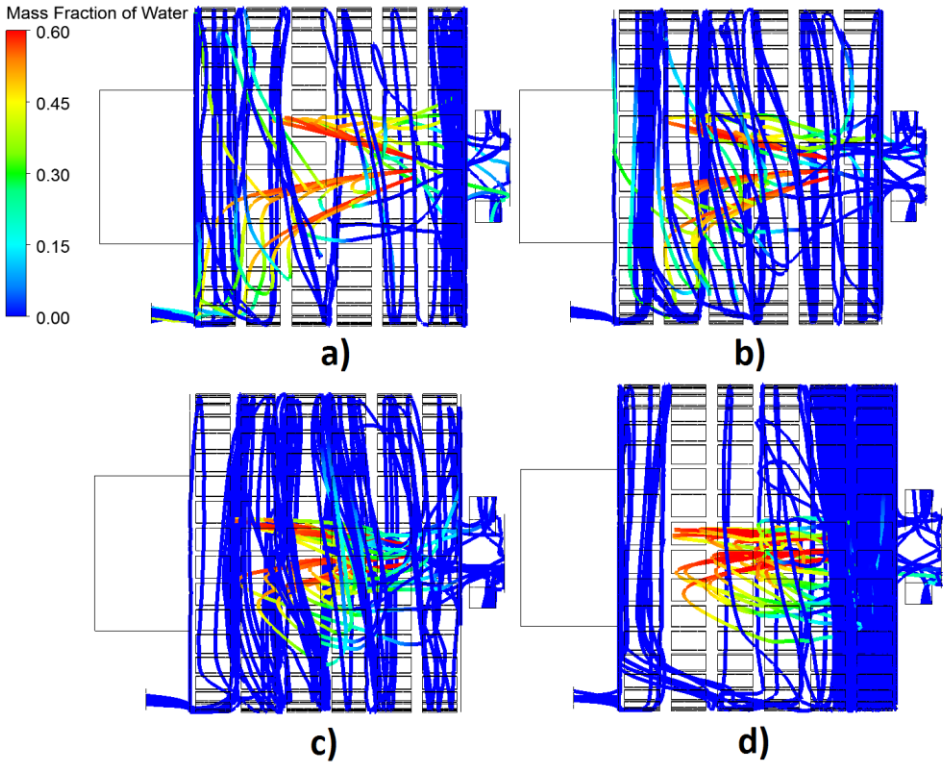

Fig.18 Particles trajectories for various spray angles: a) α = 40 °, b) α = 30 °, c) α = 20 °, d) α = 10 °. Spray parameters: RR distribution 36 - 90 μm, SMD = 63 μm, V_{inj} = 55 m/s

The drying air starts to determine the particles motion after they lose their initial momentum which is defined by their mass and injection velocity. Therefore, the particles behavior in the hot zone is governed by these parameters. The first point of attention there, is the particles penetration distance to the chamber. There have to be no contact between particles and the front wall and neither with the inlet cylinder walls. Fig.19 represents particles trajectories of different sizes (Rosin-Rammler distribution: from 36 to 120 μm, spread parameter = 2.45) for the injection velocity of 55 m/s which is valid for the atomization pressure of 15 bar and respective SMD of 63 μm as follows from formulas (1) and (2). It can be seen that the particles bigger than approximately 90 - 100 μm would stick to the front plate and cylinder walls due to a large amount of moisture at the moment of contact. This implies the particles size limitation for the given chamber length. However, the SMD of 63 μm is likely to cause the presence of the particles of undesirable size. Hence, the further investigation was done for a smaller SMD.

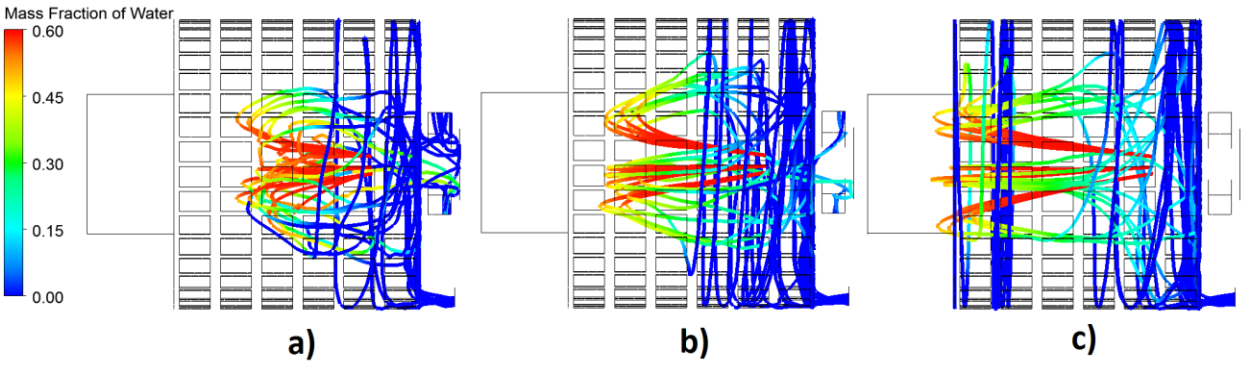

Fig.19 Particles trajectories for V_{inj} = 55 m/s and α = 20 ° : a) 36 µm < D < 60 µm, b) 60 µm < D < 90 µm, c) 90 µm < D < 120 µm

Consequently, the atomization pressure was set to 30 bar which results into V_{inj} = 77 m/s and SMD = 54 µm. Fig.20 illustrates the particles behavior for these conditions. The observed results confirm that the maximum particle size must be below 90 µm although there is a potential of drying the particles of a bigger size if they flow close to the center line (Fig.19c and Fig.20c).

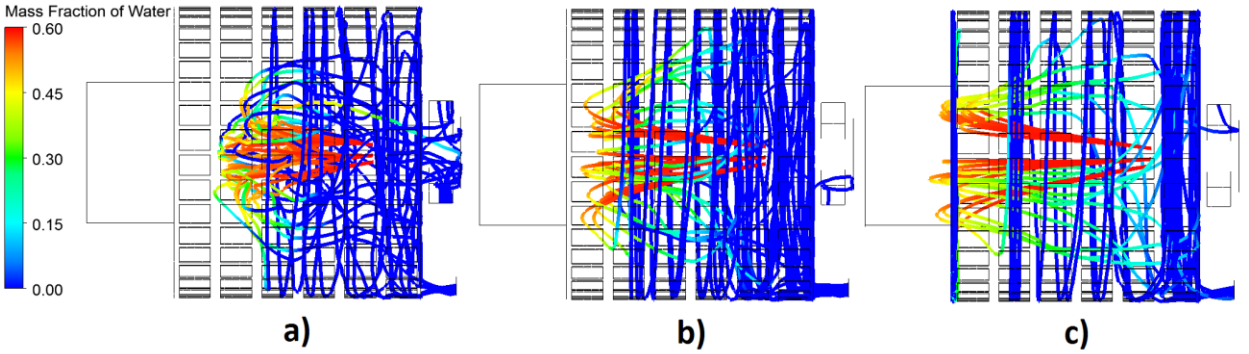

Fig.20 Particles trajectories for V_{inj} = 77 m/s and α = 20 ° : a) 36 µm < D < 60 µm, b) 60 µm < D < 90 µm, c) 90 µm < D < 100 µm

5.1.5 Influence of outlets

As it was demonstrated in Chapter 5.1.3, the increase of G-force does not lead to efficient separation. Therefore, solid outlets modifications have been tested for determining their influence on separation as well as the limits of influence. Three different number of outlets, which location is shown in Fig.21, were investigated for particles size from 30 to 90 µm with SMD = 54 µm. The results presented in Table 3 indicate that the maximal separation efficiency achieved by increasing the number of outlets is at 85 % while four outlets is the optimal number for that.

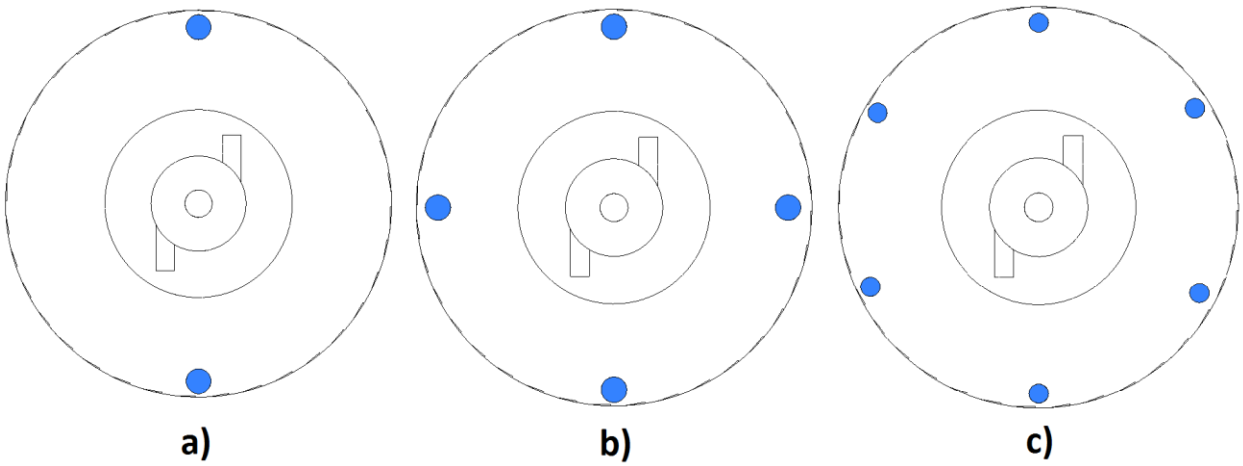

Fig.21 Solid outlets location at the back side: a) 2 outlets, b) 4 outlets, c) 6 outlets

Table 3 Separation efficiency depending on the outlets

Number of outlets	Maximal separation efficiency
1 (default)	50 %
2	75 %
4	85 %
6	85 %

In order to illustrate the impact of outlets on the flow, the velocity streamlines across the dryer with 4 solids outlets are presented in Fig.22. It can be observed that the flow in the chamber is symmetrical with the air streams directed towards each outlet. Thus, the particles both in the mixing and in the cold zones are getting entrained by flow bringing them to the solid outlets. However, the smallest particles that do not leave the hot zone are not captured by the solids outlets located on periphery but escape through the gas outlets at the center of the back side. Furthermore, one could observe a small recirculation zones between the front plate and the 1st wheel. Hence, particles presence in those zones should be minimized which is currently the case for sizes below 90 μm as can be seen in Fig.20.

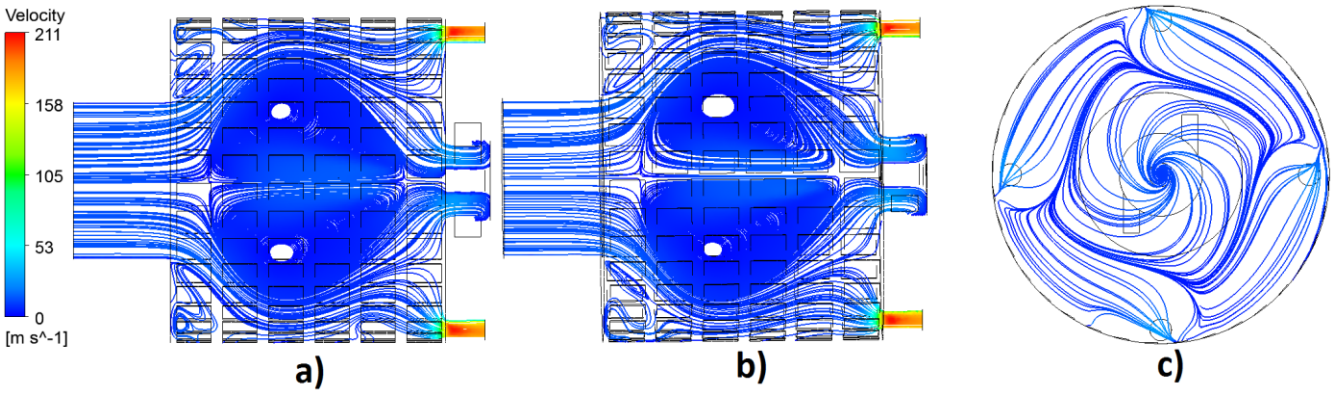

Fig.22 Velocity streamlines of the four - solids outlets configuration: a) and b) at the outlets cross-sections, c) at the 6th wheel

An alternative configuration with the solids outlet at the front plate was also tested. Although the obtained separation efficiency was in the same range as for the back side solid outlet (one outlet), a problem with the drying on the bottom part of spray was encountered. As can be seen in Fig.23, the large particles injected to the direction of the outlet are entrained by it too fast and hit the walls while still having 20 - 35 % of moisture which is not acceptable for the process.

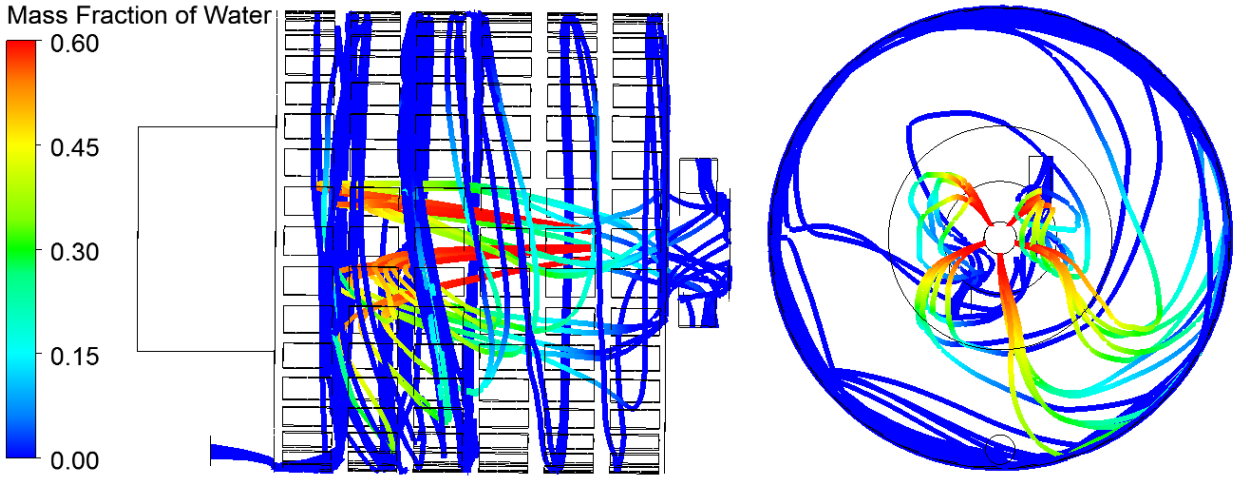

Fig.23 Drying of the particles with 70 μm < D < 90 μm in the front side outlet design. Spray parameters: RR distribution 30 - 90 μm, SMD = 63 μm, V_{inj} = 55 m/s

5.1.6 Capacity investigation

The spray dryer capacity signifies the amount of spray feed that can be entirely dried per unit of time. While undertaking the capacity tests, it is necessary to keep track of the energy efficiency that serves as the reference and the limitation factor which does not allow to exceed a certain amount of energy spent per unit of evaporated moisture. The energy efficiency in drying industry is commonly expressed by specific energy consumption E_s (kJ/kg) as follows:

$$E_s = \frac{\sum Q_{heat}}{F_e} \tag{5}$$

where Q_{heat} is the amount of heat input to dryer (kJ/h) and F_e is the amount of evaporated moisture from feed (kg/h). The amount of heat is calculated as follows (*da Silva et al., 2017*):

$$Q_{heat} = (c_{pa} \times T_{air} + x_s \times (h_{we} + c_{pw} \times T_{air})) \times \dot{M}_{air} \tag{6}$$

Where c_{pa} is the specific heat of air (kJ/kg°C), T_{air} is the temperature of drying air at the inlet (°C), x_s is the humidity ratio at saturation (kg/kg), h_{we} is evaporation heat of water (kJ/kg), c_{pw} is the specific heat of water (kJ/kg°C) and $\dot{M}_{air}$ is the air mass flow rate (kg/h), which corresponds to $\dot{M}_{hot}$ and $\dot{M}_{cold}$ for each flow respectively.

In order to achieve efficient drying process, it is necessary to assure a large convective heat transfer coefficient between particles and drying air. An experimentally obtained expression (*ECN, 2017*) based on dimensionless numbers was used:

$$Nu = 2 + 0.6 \times Re_p^{\frac{1}{2}} \times Pr^{\frac{1}{3}} \tag{7}$$

where Nu is Nusselt number, Re_p is the particle Reynolds number defined as $\frac{\rho U D_p}{\mu}$ and Pr is Prandtl number. Fig.24 represents Reynolds and Prandtl number evolution of injected particles. It can be seen that the average values of Re_p and Pr in the hot zone are around 200 and 0.8 respectively. Their substitution in formula (7) leads to Nu ≈ 10. The obtained value signifies a strong effect of convection on the drying process. For instance, *Tolmač et al. (2008)* reported the values of Nu between 7 and 37 for highly efficient convective drying of granular particles having average diameter of 1 mm. Hence, Nu ≈ 10 for much smaller particles indicates a comparable flow impact.

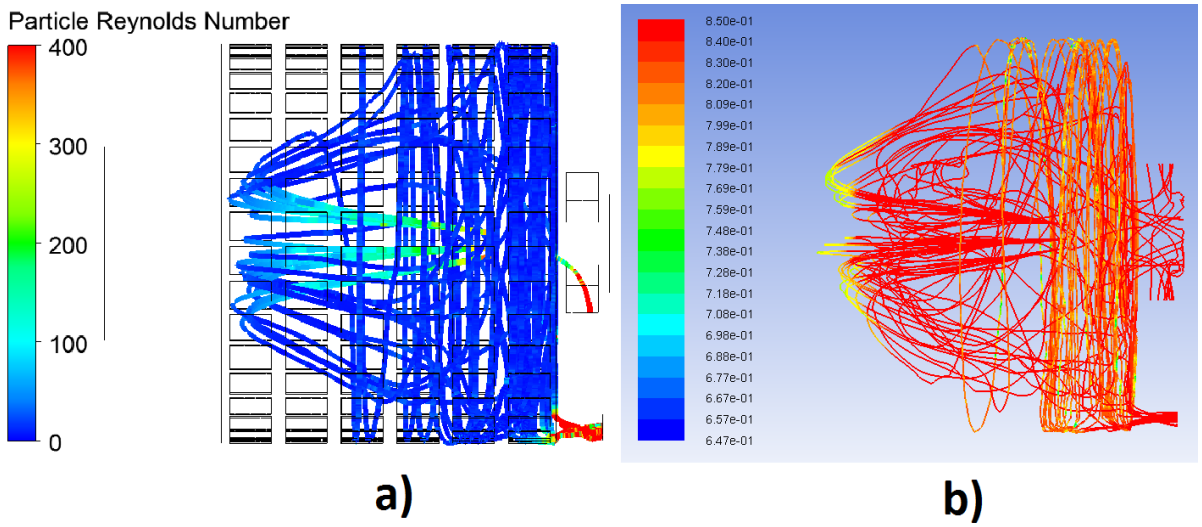

Fig.24 Dimensionless particle numbers change: a) particle Reynolds number, b) Prandtl number

As follows from the requirements, the pilot-scale plant has to be able to dry approximately 250 kg/h of feed. Since the process objective is to remove 60 % of initial moisture, this leads to F_e = 150 kg/h. Thus, the first test was performed with such an amount of feed. However, the drying of the biggest particles (80 - 90 μm) that can be seen in Fig.25a, is not complete. Many particles still have 20 - 30 % of moisture while impinging the chamber wall. This means that the temperature drop caused by evaporation of 250 kg/h of feed reduces the drying potential for the biggest particles. Therefore, a lower feed of 234 kg/h has been tested. As shown in Fig.25b, the drying became more effective so the particles have 0 - 10 % of moisture while approaching the walls. Thus, the spray feed of 234 kg/h would be the optimal one for the given dimensions and operating conditions. With the total heat input of 954 000 kJ/h, this leads to the energy efficiency of 6 800 kJ/kg. *Baker and McKenzie (2005)* reported that the average energy consumption in industrial spray dryers in food industry is about 8 000 kJ/kg. Hence, the designed system can be considered as energy efficient and ready for further improvements such as the application of heat recycling technique.

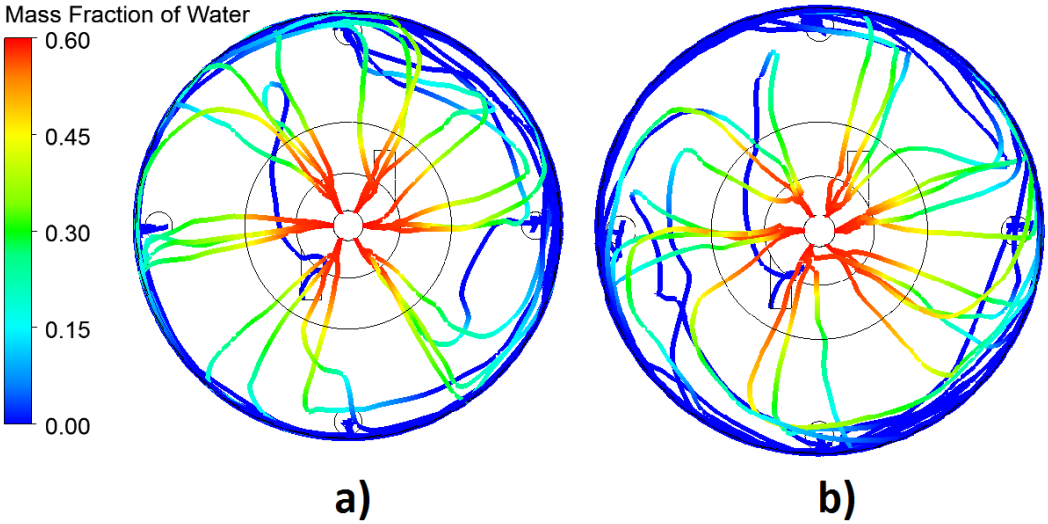

Fig.25 Drying of the particles of 80 μm < D < 90 μm: a) Q_{liq} = 250 kg/h, b) Q_{liq} = 234 kg/h
Spray parameters: RR distribution 30 - 90 μm, SMD = 54 μm, V_{inj} = 77 m/s

5.2 Summary

In overall, the presented design demonstrates the performance within the requirements. The parametric investigation demonstrated several critical features in the given configuration and led to the list of optimal operating conditions and design improvements:

- hot air input of 0.5 kg/s at 390 °C;
- cold air input of 0.45 kg/s at 140 °C;
- GF = 107 g;
- nozzle is located between the wheels 5 and 6;

- Q_{liq} = 234 kg/h;
- particles size between 30 and 90 µm with SMD = 54 µm and V_{inj} = 77 m/s;
- four solids outlets at the back side;
- energy efficiency (E_s) of 6 800 kJ/kg of evaporated water;
- separation efficiency of 85 %.

Chapter 6

Design of Configuration 2 based on the lab-scale unit

6.1 Source design overview

As explained in Chapter 4.1.2, the second design is based on an optimized laboratory-scale unit. Its performance and operating conditions are presented herewith as the reference for up-scaling procedure which target is to maintain the same functioning on a bigger scale.

The hot air is introduced through the cylinder with flow rate of 0.186 kg/s at 350 °C. The cold air injection is not uniform over the chamber and changes both in terms of flow rates and temperature as shown in Table 4.

Table 4 Cold air injection parameters

Wheel number	Flow rate, kg/s	Temperature, °C
1	0.0425	110
2	0.0425	110
3	0.0450	110
4	0.0450	110
5	0.0375	105
6	0.0375	105

The nozzle is located at the level of the left edge of the wheel 2. Thus, the drying is supposed to occur in the cylinder while the vortex chamber serves as a particle separator. The optimized nozzle parameters *(Jamil Ur Rahman, 2018)* are as follows:

- particles size from 40 to 90 μm with SMD = 52 μm;
- V_{inj} = 70.7 m/s;
- T_{feed} = 67 °C;
- spray angle α = 20.5 °;
- $\dot{M}_f$ = 56 kg/h.

The particles trajectories are represented in Fig.26. It can be seen that the drying is accomplished for all sizes. However, some of the biggest particles are hitting the cylinder wall before the drying is complete which is considered as the only drawback of the source design. It is also visible that only a part of the smallest particles is leaving through the gas outlets. Consequently, the resulted separation efficiency is at 90 - 95 %. The feed rate of 56 kg/h corresponds to 33.5 kg/h of evaporated water and leads to energy efficiency E_s = 7 000 kJ/kg. More details can be found in the work of *Jamil Ur Rahman (2018).*

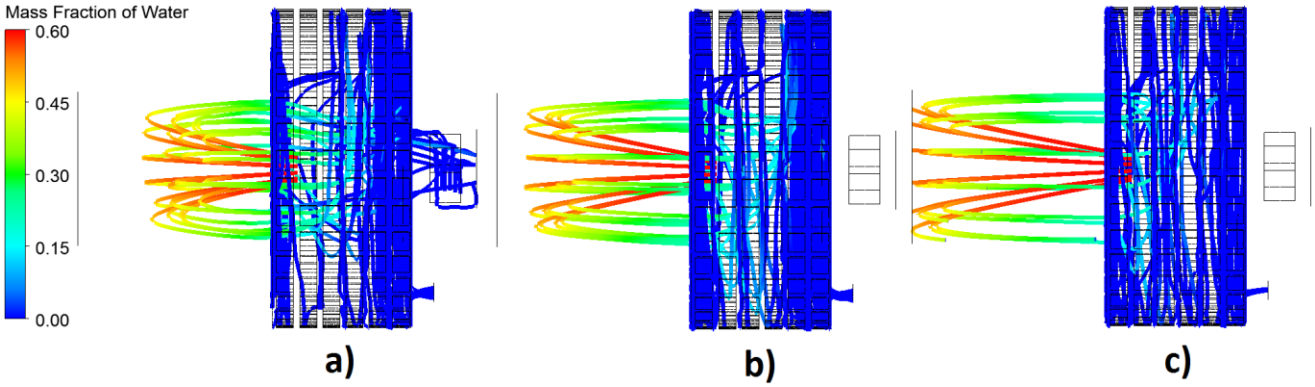

Fig.26 Particles trajectories in the optimized lab-scale design: a) a) 40 µm < D < 60 µm, b) 60 µm < D < 75 µm, c) 75 µm < D < 90 µm (*Jamil Ur Rahman, 2018)*

6.2 Parametric analysis

In a similar way as for Configuration 1, influence of various parameters was examined. As explained in Chapter 4.1.2, the volume of Configuration 2 is equal to the Configuration 1 volume.

6.2.1 Velocities projection

The first scaling up approach was to keep the same velocities in the dryer which are 10.5 m/s for hot air and 25 - 31 m/s for cold air. Thus, such velocities were imposed by adjusting the flow rates. It can be seen from Fig.27 that the hot air velocity is not sufficient for assuring the plug flow in the cylinder - the cold air penetrates to the cylinder which has to be avoided. On the other hand, drying is almost complete by the moment of contact between particles and the chamber walls. However, the obtained separation efficiency is only at 34 % which is due to insufficient velocities of the cold air.

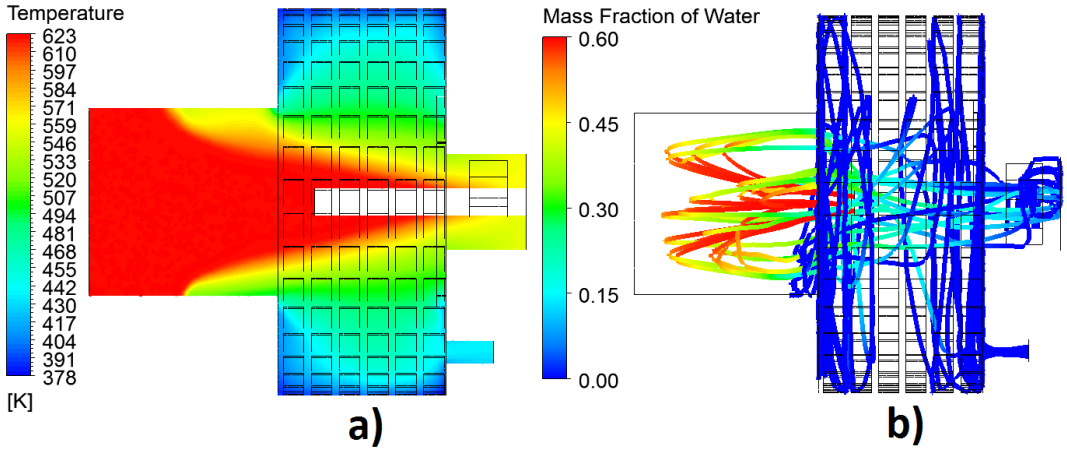

Fig.27 Results for the case with the same velocities as on the small scale:
a) temperature contour without spray, b) particles trajectories

Therefore, in order to improve the separation, the G-force was also scaled by factor 1.8 relatively to the initial values of the source design (360 - 475 g). This corresponds to the velocities of 46 - 56 m/s for generating the G-force of 580 - 860 g on the bigger scale. As expected, the obtained cold air recirculation is more pronounced (Fig.28a) and more particles are entrained by the vortex flow (Fig.28b), which leads to the separation efficiency of 55 %.

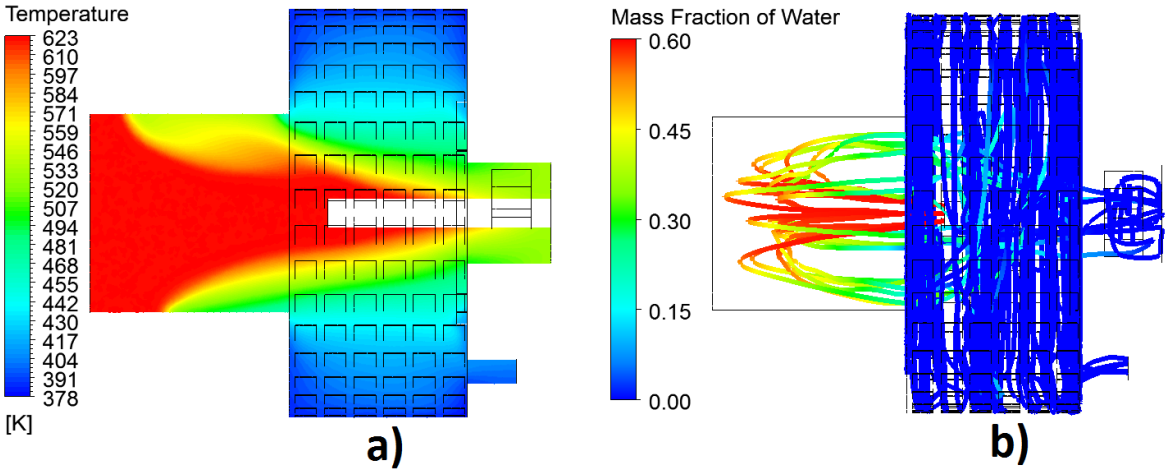

Fig.28 Results for the case with the initial hot air velocity and scaled G-force:
a) temperature contour without spray, b) particles trajectories

The next step was to impose the plug flow in the cylinder such that no backflow from the chamber is present there. Therefore, the hot air flow rate was increased by 20, 40 and 60 % from the nominal one. As can be observed in Fig.29, the case with increase by 40 % still involves a small recirculation in the cylinder. However, the increase by 60 % is too expensive in terms of energy, thus the flow rate rise by 40 % was chosen for further simulations. Another reason for that is the concept of particles drying in the cylinder while + 60 % case generates unnecessarily large hot zone in the chamber.

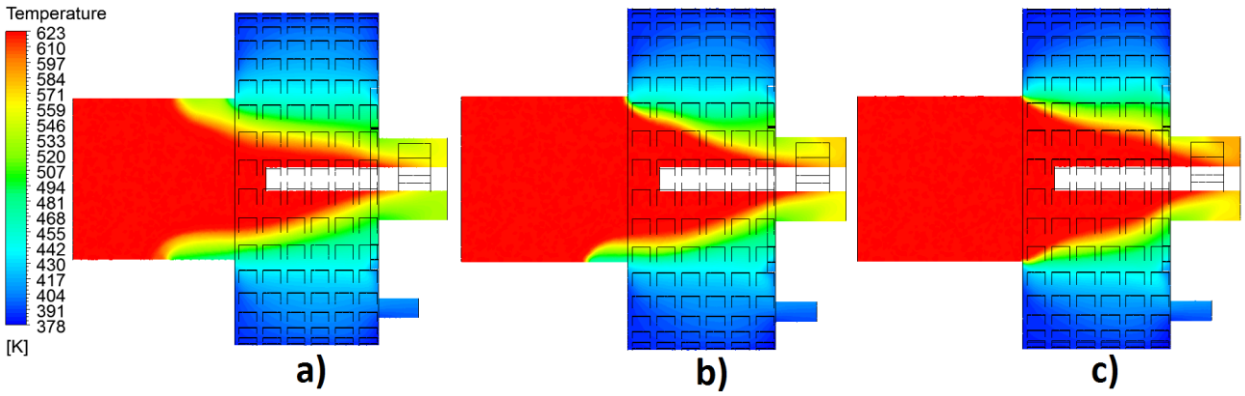

Fig.29 Temperature contours for hot air flow rates changes: a) +20 %, b) + 40 %, c) + 60 %

The particle trajectories for the 40 % hot air increase are shown in Fig.30. The profile indicates that the particles of average and big size are not completely dried while impinging the back side of the chamber. This can be a result of a too high value of spray feed that was adapted to the energy input. Therefore, the capacity investigation will be presented for this design as well. Apart from drying issues, the obtained separation is as follows:

- 50 % at the solids outlet;
- 43 % at the gas outlets;
- 7 % impinging the cylinder wall.

This implies that in parallel with separation improvement, there must be found a way to avoid the contact of sprayed particles and the cylinder wall.

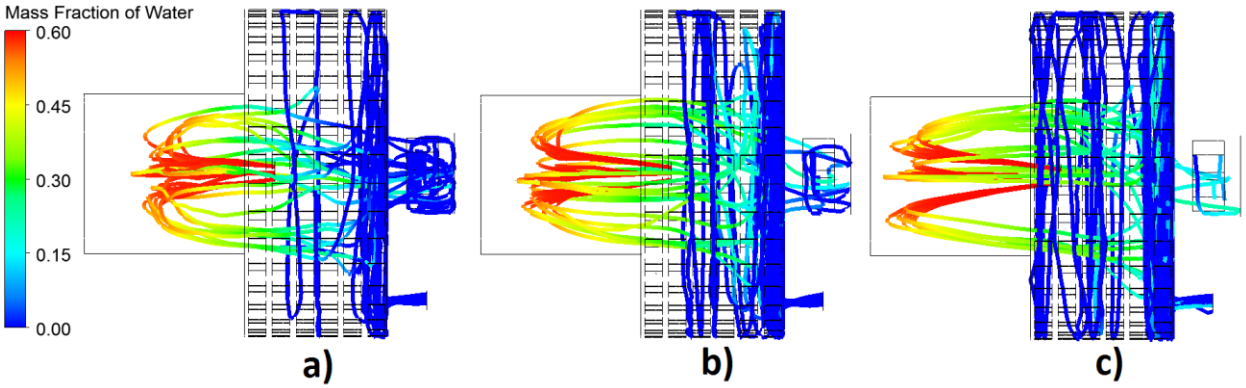

Fig.30 Particles trajectories for the case with +40 % of hot air flow rate and $\dot{M}_f$ = 468 kg/h:
a) 40 µm < D < 60 µm, b) 60 µm < D < 75 µm, c) 75 µm < D < 90 µm

6.2.2 Influence of G-force

Since the resulted separation efficiency from application of the originally designed G-force is only around 50 %, the flow was locally increased for investigating its influence on the separation. Table 5 represents the details of undertaken simulations. It can be observed that even major values of G-force, i.e. around 1350 g resulted from the cold air injection velocity of 70 m/s do not lead to efficient separation on a bigger scale. Hence, the G-force impact in Configuration 2 is similar to the one presented for Configuration 1 in Chapter 5.1.3 - it has a limited and nonlinear influence on the separation process.

Table 5 G-force increase tests for Configuration 2

Relative flow rate increase	G-force	Separation efficiency
+ 20 % uniformly	840 - 1240 g	52 %
+ 40 % at the wheels 1 and 2	1350 g	58 %

6.2.3 Contact of particles and the cylinder wall

As follows from the simulation which results are shown in Fig.30, the amount of particles impinging the cylinder wall is at 7 % of the total number, although the cylinder is 1.8 times bigger compared to the small scale. Due to a large moisture content, the particles will stick to the walls and therefore this phenomenon should not be present in the process. First, the influence of spraying angle was investigated. Thus, the initial angle $\alpha = 20.5\ °$ was decreased in order to make the injection even more narrow and avoid the particle-wall contact in that way. The trials results given in Table 6 match again the trends observed in Configuration 1 - decreasing of spray angle is beneficial only until a certain limit, after which it is problematic to predict the particles behavior.

Table 6 Spray angle change results

Spray angle	Amount of particles impinging the cylinder wall
16°	7 %
12°	25 %
8°	25 %

In the similar manner, the spray feed was gradually decreased from $\dot{M}_f = 468$ kg/h which is the amount imposed according to formulas (5) and (6) in order to stay in the energy efficient range. As can be seen in Table 7, the major reason for particles approaching the cylinder wall is the spray feed that has a significant impact on the air flow at high values. Consequently, the concept of drying in the cylinder has strict limitations in terms of spray feed. In the given configuration, the safe value is 216 kg/h which is far below the reference for energy efficiency. With the total energy input to the dryer of 1 418 000 kJ/h and the evaporation of 129.6 kg/h, the resulted energy efficiency is equal to 10 940 kJ/kg that is considerably lower compared to the one in Configuration 1. However, if there was no limitation related to particle-wall contact, the efficiency might be increased to 6 000 - 7 000 kJ/kg.

Table 7 Spray feed change results

Spray feed	Amount of particles impinging the cylinder wall
324 kg/h	7 %
288 kg/h	0.5 %
252 kg/h	0.1 %
216 kg/h	none

6.2.4 Influence of outlets

Since the separation efficiency remains moderate even in the presence of a strong centrifugal force, the alternative way for its improvement is adding more solids outlets as was shown for Configuration 1. Thus, three different cases were considered: one outlet with increased size, two outlets and four outlets as shown in Fig.31, with the following constant parameters: α = 20.5 °, $\frac{\dot{M}_{hot}}{\dot{M}_{cold}}$ = 1.04, GF = 580 - 860 g, $\dot{M}_f$ = 216 kg/h. The results for each case are given in Table 8.

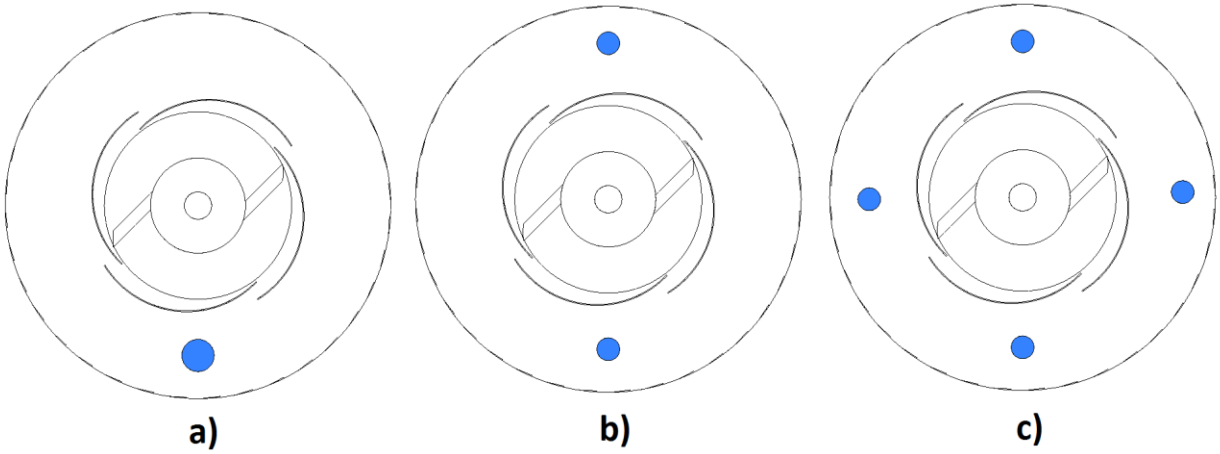

Fig.31 Solids outlets location: a) 1 larger outlet, b) 2 outlets, c) 4 outlets

Table 8 Separation efficiency depending on the outlets

Case	Separation efficiency
1 larger outlet	45 %
2 outlets	45 %
4 outlets	35 %

Unexpectedly, the increase of outlets number did not lead to the separation improvement. However, the velocities streamlines represented in Fig.32 explain poor separation efficiency of Configuration 2 in general. It can be seen that there are large recirculation zones all over the chamber corners. Consequently, the vortex flow does not closely interact with the hot zone so the particles do not get entrained towards periphery. Although the hot air flow is not as fast as the cold air flow (15 m/s against 46 - 56 m/s respectively) and the ratio between them is equal to 1.04, the hot air streams' preferred path is towards the gas outlets. This can be explained by the absolute distance between periphery and the center of the dryer. The chamber diameter of Configuration 2 is 0.742 m against 0.618 m in Configuration 1, thus the particles drying zone might be too far from both the vortex flow and the solids outlets. If this assumption is correct, it would impose serious limitations on the scaling up of the vortex chamber spray dryer due to the impossibility to develop a large industrial-scale unit.

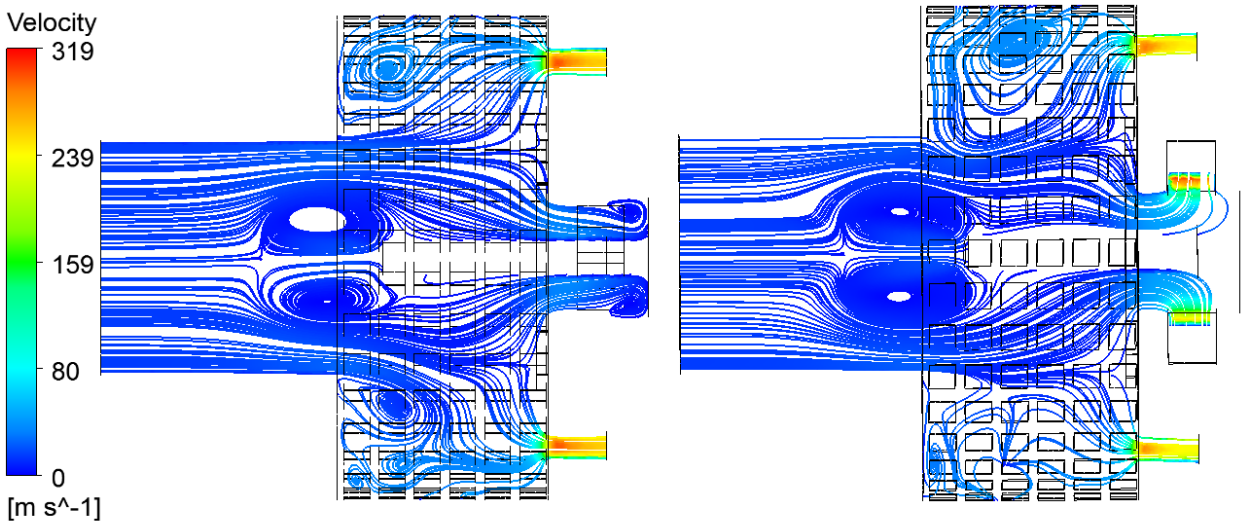

Fig.32 Velocities streamlines for four solid outlets case

6.3 Summary

The scaling up procedure of the presented design ended up with the following operating conditions and design changes:

- hot air input of 0.844 kg/s at 350 °C;
- cold air input of 0.81 kg/s at 105 - 110 °C;
- GF = 580 - 860 g;
- nozzle is located between the wheels 1 and 2;
- capacity ($\dot{M}_f$) of 216 kg/h;
- particles size between 40 and 90 μm with SMD = 54 μm and V_{inj} = 77 m/s;
- 1 solid outlet at the back side;
- energy efficiency (E_s) of 10 940 kJ/kg of evaporated water;
- separation efficiency of 50 %.

It can be thus concluded that neither efficient drying nor the separation was achieved on the bigger scale for Configuration 2. Moreover, it was discovered that spray drying in the cylinder imposes limitations on the feed flow rate that makes the process substantially inefficient. However, general findings about the vortex chamber spray dryer performance and its scaling up aspects have been identified by investigating Configuration 2.

Chapter 7

Design deliverables

7.1 Design proposals overview

In Chapters 5 and 6, two different design solutions of the pilot-scale spray dryer are proposed. Their performance comparison is provided in Table 9. Although both designs have similar capacities and spray parameters, the most crucial aspects such as the energy and separation efficiencies are significantly more advantageous in Configuration 1. In fact, the energy efficiency in Configuration 2 is restricted by the cylinder diameter that cannot be used for a bigger spray feed, while the separation efficiency could not be improved due to a large distance between the drying zone and the rotational flow. Therefore, Configuration 1 is considered as the well optimized and most promising pilot-scale design of the vortex chamber spray dryer.

Table 9 Design proposals comparison

Parameter	Configuration 1	Configuration 2
Chamber diameter	0.618 m	0.742 m
Chamber length	0.525 m	0.323 m
Cylinder diameter	0.30 m	0.36 m
Cylinder length	0.185 m	0.363 m
Volume	0.17 m^3	0.18 m^3
Number of gas outlets	2	2
Number of solids outlets	4	1
Temperature of hot air	390 °C	350 °C
Temperature of cold air	140 °C	105 - 110 °C
Gas outlets temperature	165 °C	205 °C
Solids outlets temperature	155 °C	100 °C
Flow rate of hot air	0.500 kg/s	0.844 kg/s
Flow rate of cold air	0.45 kg/s	0.81 kg/s
Nozzle position	Between the wheels 5 and 6	Between the wheels 1 and 2
Atomization pressure	30 bar	30 bar
Spray injection velocity	77 m/s	77 m/s
Droplets size	30 - 90 μm	40 - 90 μm
Spray feed	234 kg/h	216 kg/h
Total energy input	954 000 kJ/h	1 418 000 kJ/h
Energy efficiency	6 800 kJ/kg of evap. water	10 940 kJ/kg of evap. water
Separation efficiency	80 - 85 %	45 - 50 %

7.2 Economic evaluation

7.2.1 Energy cost estimation

Although the pilot-scale spray dryer is not meant yet for fully industrial exploitation, it is important to estimate the current operating cost and identify perspectives for further optimization. On the other hand, there is a certain risk that the vortex chamber spray dryer cannot be up-scaled to industrial size, so the alternative in that case would be using multiple pilot-scale size units in parallel. Therefore, the following estimation is made by applying the industrial process criteria.

One operational year for spray drying of food products corresponds to 6 000 hours and requires in average of 8 000 GJ/t water evaporated (*Mercer, 1986*). The proposed design requires of 954 000 kJ/h that corresponds to 265 kW of heat. The price for non-household consumers in the Netherlands by November 2017 is equal to 87 euro per MW (*Electricity price statistics, 2017*). Thus, the energy cost of one operational year would be around 140 000 euro. Since the current improvement relatively to the average energy consumption in spray dryers is at 15 % (6 800 GJ/t against 8 000 GJ/t), the potential savings are at 25 000 euro per year for one pilot-scale unit. The total amount of milk powder produced in the Netherlands in 2016 is equal to 233 000 tons (*Netherlands Enterprise Agency, 2018*), which energy consumption cost for spray drying is approximately equal to 68 million euro. Thus, potential 15 % savings from using the vortex chamber drying technology would globally result in 10 million euro per year for the current production rate.

7.2.2 Heat regeneration potential

The main opportunity for energy saving in the vortex chamber spray dryer comes from the heat regeneration option. Although the quantity of heat recovery is driven by many factors, it is mainly determined by temperature parameters *(Ai et al., 2016)*. A relatively high temperature at the gas outlets (165 °C in the proposed design) thus opens perspectives of its efficient use. The heat pump system with two heat exchangers (Fig.33) can be used for cooling down the exhaust air stream from the dryer and using the obtained energy for heating up the inlet stream(s).

An in-depth study of heat recovery in various spray dyers was carried out by *Vanslambrouck (2017)*. The undertaken simulations of drying optimization predicted the reduction of specific energy consumption by 11 - 60 % depending on the heat regeneration system. For instance, a standard heat pump configuration in a conventional spray dryer demonstrated the reduction of E_s by 25 %. Therefore, implementation of heat recovery system with such a performance may lead to the total energy cost reduction from 58 to 43 million euro per year.

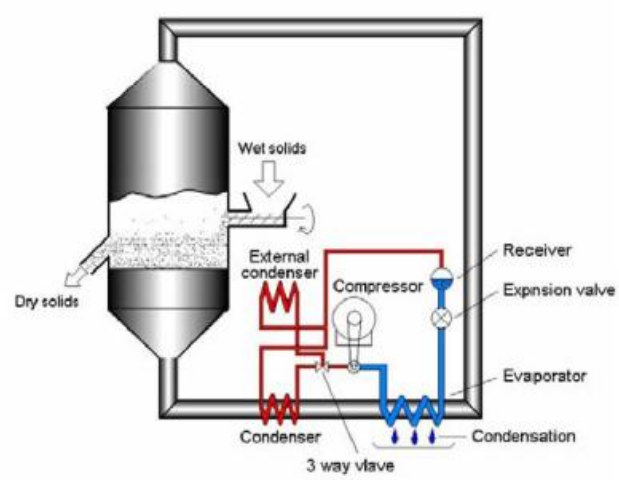

Fig.33 Scheme of the heat pump fluidized bed dryer (*Law and Mujumdar, 2007*)

7.2.3 Construction cost estimation

In order to calculate the construction and installation cost, Aspen Capital Cost Estimator V10 was used. Although the smallest spray dryer available in its library is the one with evaporation capacity of 320 kg/h and 3 m in diameter, it was chosen for identifying the cost of an industrial plant with such dimensions.

Thus, the following data was taken into account:

- spray drying system including dryer, compressor, heater, heat exchanger, piping, etc.;
- inlet gas temperature of 390 °C;
- evaporation capacity of 320 kg/h;
- dryer diameter of 3 m;
- plant location: Rotterdam, NL.

The obtained capital cost estimation is represented in Table 10. It can be seen that the equipment and setting costs are making only a half of the total cost. Electrical system items (cables, transformers, generators, etc.) and instrumentation (measuring devices, valves, regulators, etc.) also consist a significant part in the required budget.

Table 10 Capital costs summary

Item	Material (EUR)	Manpower (EUR)	Percentages
Equipment & Setting	438 000	12,032	50.6
Piping	22 515	10,514	3.7
Civil	5 423	10,904	1.8
Structural Steel	2 577	1,073	0.4
Instrumentation	101 489	10,197	12.6
Electrical	195 324	55,713	28.2
Insulation	10 306	11,315	2.4
Paint	171	1,598	0.2
Subtotal	**775 805**	**113 347**	**100**
Total material and manpower cost: EUR 889 152			

The overviewed spray dryer with the evaporation capacity of 320 kg/h would lead to production of 1 280 ton of milk powder per year and thus to a need of 182 units for the production of 233 000 ton per year. Assuming a similar construction cost of the industrial-scale vortex chamber spray dryer units, their total construction cost would be equal to 162 million euro. By considering a yearly amount of saved energy corresponding to 25 million euro, the payback period would be equal to 7 years.

7.2.4 Technology Readiness Levels

Technology Readiness Levels (TRL) is a methodology for estimating maturity of new technologies. Developed during 1970 – 80s by the National Aeronautics and Space Administration (NASA) for space programs, it is widely used today for decision making on R&D investments at EU level *(EARTO Recommendations, 2014)*.

Readiness levels from 1 to 9 are described in Fig.34. Although the right column is related to aerospace engineering, it can be easily projected to other technologies.

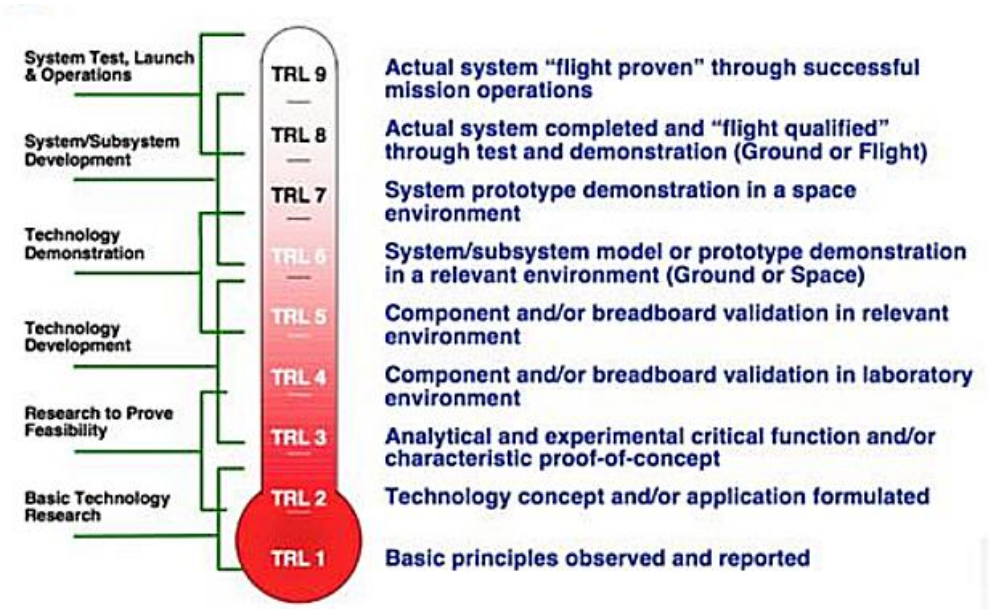

Fig.34 NASA TRL scale *(EARTO Recommendations, 2014)*

The designed vortex chamber spray dryer corresponds to the Technology Demonstration levels while being still in the Technology Development phase. Therefore, the current readiness level is 6 which is characterized by system model demonstration in an operational environment. In case of a successful physical prototype operation (best case scenario), the readiness level 7 will be achieved and the system will be tested and optimized further in various conditions. On the other hand, absence of model predicted performance (worst case scenario) would move the progress back to the level 4. In that case, the lab-scale unit would have to be studied again in parallel with a general feasibility research.

Chapter 8

Conclusions and recommendations

8.1 Conclusions

General findings

The general objectives of the design project stated in Chapter 1.3 have been achieved. Namely, the CFD model was specified and validated, the pilot-scale unit was designed and optimized and the obtained solution was evaluated.

The design of spray dryer can be successfully accomplished by means of CFD modelling. Although experimental tests are necessary, the complexity of physical phenomena occurring in the dryer makes the empirical design procedure extremely difficult. In fact, the designed process involves turbulent mixing of air of various temperatures, multiphase interactions (gas, liquid, solid) and evaporation. It is very difficult to measure the mentioned parameters precisely which implies that experiments represent the grey box testing i.e. the one with an essentially limited data on the studied process.

The key aspect in spray drying process is the interaction of spray and drying air. This is not determined uniquely by the air flow but also by droplets size, injection velocity, feed rate and spray angle. Therefore, the knowledge on exact nozzle performance is prerequisite while designing a spray drying system.

Up-scaling of spray dryer has a non-linear character and generally does not lead to an efficient projection of all phenomena on a bigger scale. Hence, there is a risk that a multifunctional system such as the vortex chamber dryer will be less performant in scaled-up version. In order to minimize that risk, the designed system has to be as simple as possible in terms of the number of input variables and geometrical complexity.

Numerical simulations revealed a very high sensitivity of the vortex chamber dryer to slight changes in any of major process parameters. This signifies the necessity of CFD modelling not only for developing an approximated design but also for process optimization that requires a fine tuning for achieving a desired performance.

The designed Configuration 1 mostly satisfies the requirements listed in Chapter 2. The main parameter to optimize is the separation efficiency which is a little below the required one. Possible solutions for improvement are given in recommendations.

Detailed conclusions

The concept of spray drying in the cylinder and using the chamber for separation (Configuration 2) did not show potential on the bigger scale. Namely, large spray feed rates could not be accommodated in the cylinder without the contact between droplets and cylinder walls which would result in stickiness. This puts a significant limitation on the drying capacity and therefore on the energy efficiency.

Narrow spray angle demonstrated a deeper penetration of droplets into the chamber and a longer residence time in the hot zone. The optimal value obtained from parametric study is $\alpha=20°$ for hollow cone injection.

G-force on bigger scale has to be far stronger for picking up the particles from the hot zone. This leads to a higher amount of cold air in the dryer which is unacceptable. Thus, the separation was improved through changing the flow pattern by adding more solids outlets at the periphery level (Configuration 1). However, such an approach did not work in Configuration 2 which might be due to a large distance between the hot zone and periphery. Therefore, that aspect needs a more detailed study. If the stated assumption is right, the up-scaling to industrial size would not be possible within the current design concept.

Large particles have tendency to move to periphery and thus being separated from the air flow while smallest ones generally flow together with air and escape through the gas outlets.

According to obtained results, the designed process has the energy efficiency in industrial range. Furthermore, applying of heat regeneration technique has a potential of reducing the current energy consumption by 11 - 60 %.

8.2 Recommendations

The used CFD model simulated the process as adiabatic i.e. no heat losses to environment were taken into account. Therefore, the physical plant has to be thermally insulated in order to obtain the predicted performance. Otherwise, the modelling results must be considered as over predicting which would result in a lower dryer capacity and energy efficiency.

Counter-current spray injection against a strong air flow may lead to the nozzle clog by a large amount of deflected droplets. Therefore, the nozzle must be equipped with an additional device to avoid that. For instance, nozzles with protective caps are available in the market.

In practice, the total solids outlets surface area might be too large and result in a significant amount of exhaust gas together with powder. In such case, the product outlets size reduction would be a possible option.

As it was mentioned in conclusions, the smallest particles tend to escape through the gas outlets. This problem can be avoided by spraying larger droplets which would also lead to a re-design of the dryer. Since the major issue with the big droplets was their contact with the front chamber side, the horizontal extension of the chamber would increase the droplets size range that can be dried and more efficiently separated.

Finally, the experimental study with particles trajectories tracking is necessary for a complete model validation and understanding of the process. Moreover, the designed dryer accommodates a large spray feed in a compact volume which can lead to droplets agglomeration. Since particle-particle interaction is not calculated by the model, the experimental investigation on the particles agglomeration could give more insights about the process.

Appendix 1. Grid independency tests for Configuration 2

The characteristic lines for the grid independency tests were taken as shown in Fig. 35.

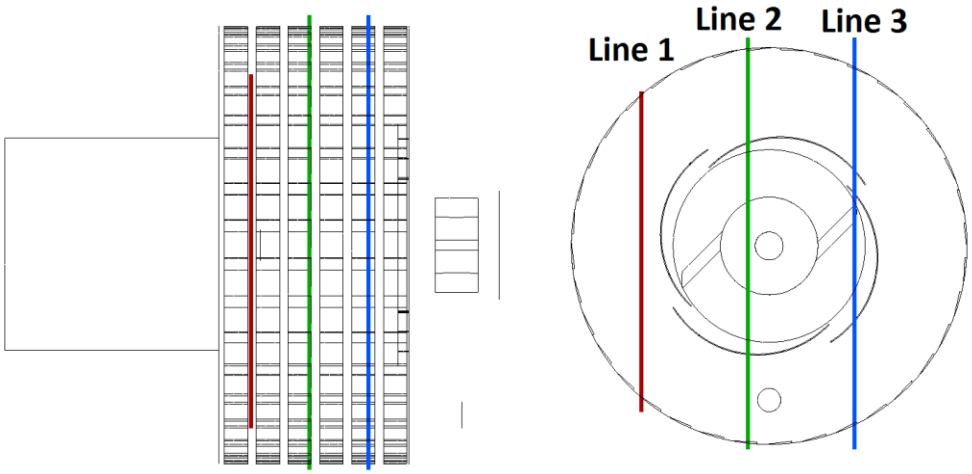

Fig.35 Characteristic lines location

Three different mesh sizes were tested: 3 M, 6 M and 9 M cells. The resulted temperature profiles over the characteristic lines are presented in Fig. 36 – 38.

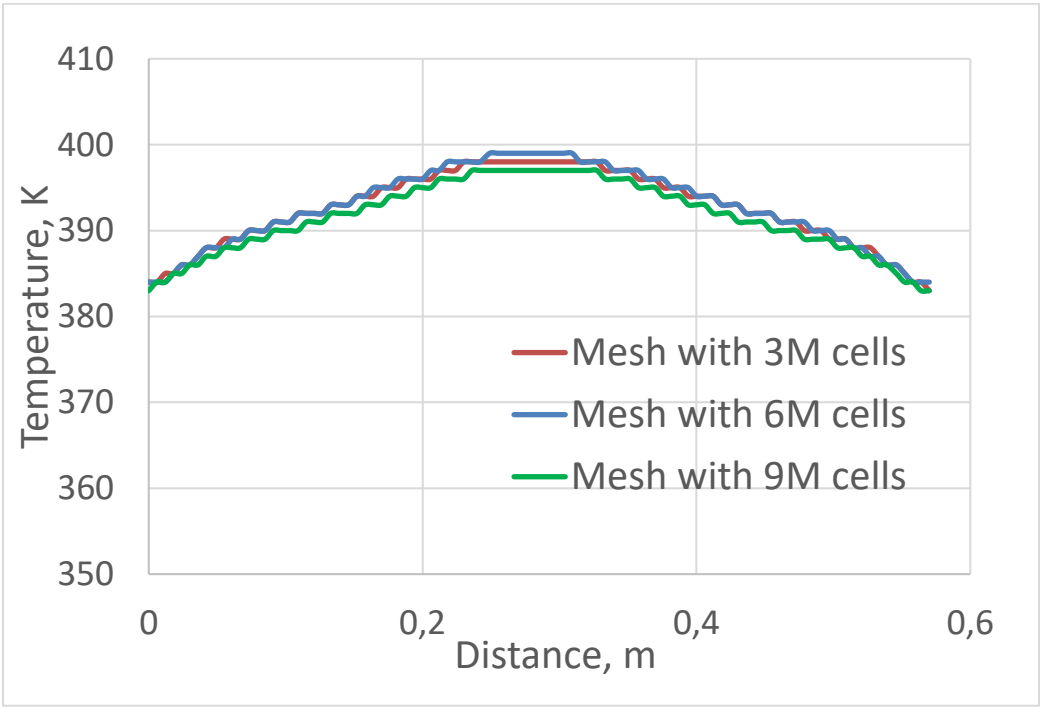

Fig.36 Temperature profile over the Line 1

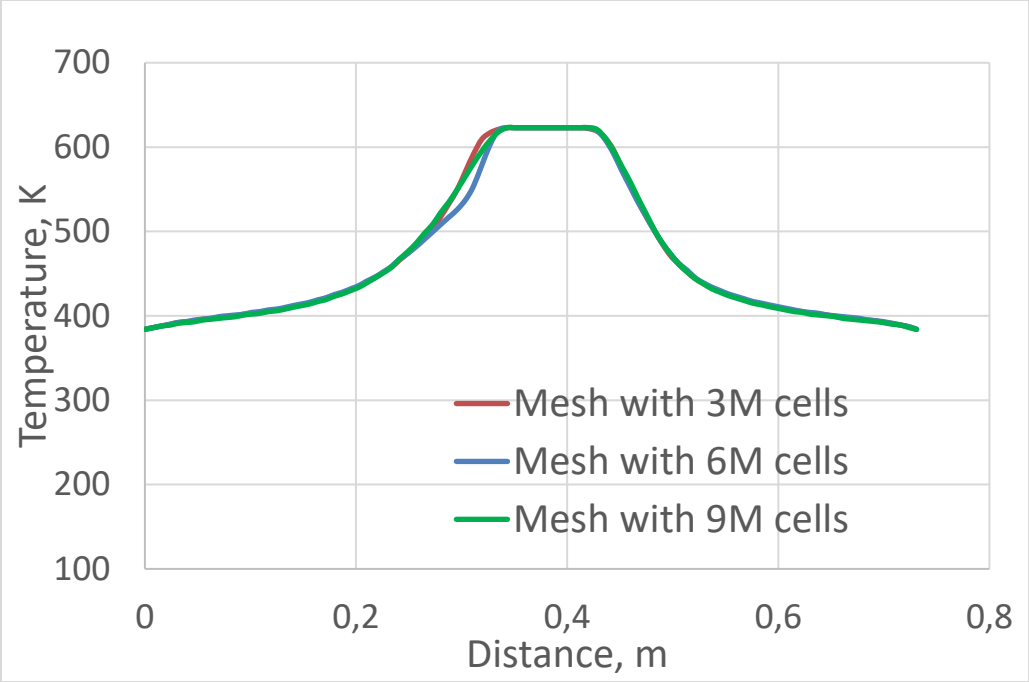

Fig.37 Temperature profile over the Line 2

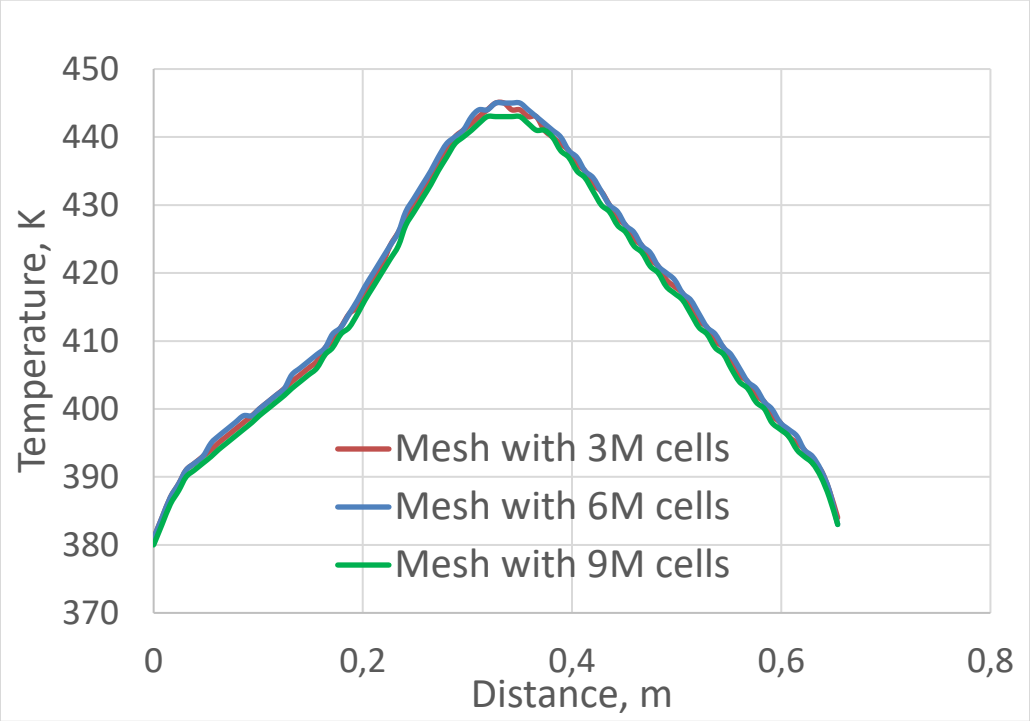

Fig.38 Temperature profile over the Line 3

References

Ai, S.; Wang, B.; Li, X.; Shi, W. Analysis of a heat recovery system of the spray-drying process in a soy protein powder plant, Applied Thermal Engineering 103 (2016), 1022 - 1030

Ali, M.; Mahmud, T.; Heggs, P.J.; Ghadiri, M.; Bayly, M.; Ahmadian H.; de Juan, L.M. CFD Simulation of a Counter-Current Spray Drying Tower with Stochastic Treatment of Particle-Wall Collision, Procedia Engineering 102 (2015), 1284 - 1294

ANSYS FLUENT 12.0 User's Guide, ANSYS, Inc. (2009)

Arpagaus, C.; Schwartzbach, H. Scale-up from bench-top research to laboratory production, Büchi Information Bulletin 52 (2008)

Baker, C.G.J.; McKenzie, K.A. Energy Consumption of Industrial Spray Dryers, Drying Technology 23 (2005), 365 - 386

Birchal, V.S.; Passos, M.L.; Wildhagen, G.R.S.; Mujumdar, A.S. Effect of Spray-Dryer Operating Variables on the Whole Milk Powder Quality, Drying Technology 23:3 (2005), 611 - 636

De Wilde, J. Gas-solid fluidized beds in vortex chambers, Chemical Engineering and Processing 85 (2014), 256–290

De Wilde, J.; de Broqueville, A. Experimental Investigation of a Rotating Fluidized Bed in a Static Geometry, Powder Technology 183-3 (2008), 426 – 435

EARTO (European Association of Research and Technology Organisations) Recommendations - The TRL Scale as a Research & Innovation Policy Tool (2014)

Electricity price statistics (2017), Link to the website:
http://ec.europa.eu/eurostat/statisticsexplained/index.php/Electricity_price_statistics

Eliaers, P.; de Broqueville, A.; van Hengstum, T.; Poortinga, A.; De Wilde, J. High-G, low-temperature coating of cohesive particles in a vortex chamber, Powder Technology 258 (2014), 242 - 251

Fletcher, D.F.; Guoa, B.; Harvie, D.J.G.; Langrish, T.A.G.; Nijdam, J.J.; Williams, J. What is important in the simulation of spray dryer performance and how do current CFD models perform? Applied Mathematical Modelling 2006, 30, 1281 - 1292

Francia, V.; Martin, L.; Bayly, A.E.; Simmons, M.J.H Influence of wall friction on flow regimes and scale-up of counter-current swirl spray dryers, Chemical Engineering Science 134 (2015), 399 - 413

Gil, M.; Vicente, J.; Gaspar, F. Scale-up methodology for pharmaceutical spray drying, Chemistry Today vol. 28 (2010), 18 - 22

Gimbun, J.; Muhammad, N.I.S.; Law, W.P. Unsteady RANS and detached eddy simulation of the multiphase flow in a co-current spray drying, Chinese Journal of Chemical Engineering 23 (2015), 1421 - 1428

Gretz Zabia L. Design of the milk spray in a novel vortex chamber dryer, PDEng report, University of Twente (2015)

Hou, Y.; Tao, Y.; Huai, X.; Guo, Z. Numerical characterization of multi-nozzle spray cooling, Applied Thermal Engineering 39 (2012), 163 - 170

Jamil Ur Rahman, U. Design of an optimum operational window for a novel vortex chamber spray dryer, PDEng report, University of Twente (2018)

Jaskulski, M.; Wawrzyniak, P.; Zbiciński, I. CFD Model of Particle Agglomeration in Spray Drying, Drying Technology 33:15-16 (2015), 1971 - 1980

Kerkhof P.J.A.M. The role of the theoretical and mathematical modelling in scale-up, Drying Technology 12 (1994), 1 - 46

Kieviet, F.G.; Modelling Quality in Spray Drying, Ph.D. Thesis, Eindhoven University of Technology, Netherlands, 1997

Klaassen, M. Near field atomization in pressure swirl nozzles, Master thesis, University of Twente (2016)

Lal, S.; Lucci, F.; Defraeye, T.; Poulikakos, L.D.; Partl, M.N.; Derome, D.; Carmeliet, J. CFD modeling of convective scalar transport in a macroporous material for drying applications, International Journal of Thermal Sciences 123 (2018), 86 - 98

Law, C., Mujumdar, A.S. Fluidized bed dryers. Handbook of industrial drying, 3rd edn (2007)

Li, X.; Zbiciński, I. A Sensitivity Study on CFD Modeling of Cocurrent Spray-Drying Process, Drying Technology 23:8 (2006), 1681 - 1691

Masters K. Current Market-Driven Spray Drying Development Activities, Drying Technology 22:6 (2004), 1351 - 1370

Mercer, A.C. Improving the energy efficiency of industrial spray dryers, Heat Recovery Systems 6-1 (1986), 3 - 10

Milk powder production in the Netherlands from 2013 to 2016, Netherlands Enterprise Agency: Productschap Zuivel (2018), Link to the website: https://www.statista.com/statistics/722373/milk-powder-production-in-the-netherlands-by-type

Montazeri, H.; Blocken, B.; Hensen J.L.M. Evaporative cooling by water spray systems: CFD simulation, experimental validation and sensitivity analysis, Build. Environ. 83 (2015) 129 - 141

Nath, S.; Satpathy, G.R. A Systematic approach for investigation of spray drying processes, Drying Technology 16:6 (1998), 1173 - 1193

Ozmen L.; Langrish T.A.G. An experimental investigation of the wall deposition of milk powder in a pilot-scale spray dryer, Drying Technology 21 (2003) 1253 - 1272

Reh, C.; Bhat, S.N.; Berrut, S. Determination of water content in powdered milk, Food Chemistry 86 (2004), 457 - 467

Robjer Gullman, S.E.H. Development of evaporation models for CFD for application within drying process simulation, Master of Science thesis, Chalmers University of Technology (2010)

Sagadin, G.; Hriberšek M. A multistage spray drying model for zeolite 4A – water suspensions in a counter-current spray dryer, International Journal of Heat and Mass Transfer 108 (2017), 1220 - 1228

Sharma, A.; Jana, A.H.; Chavan, R.S. Functionality of Milk Powders and Milk-Based Powders for End Use Applications - A Review, Comprehensive reviews in food science and food safety 11 - 5 (2012), 518-528

da Silva, C.R.; Martins, E.; Pereira Silveira, A.C.; Simeão, M.; Lessa Mendes, A.; Tuler Perrone, I.; Schuck, P.; de Carvalho, A.F. Thermodynamic characterization of single-stage spray dryers: Mass and energy balances for milk drying, Drying Technology 35:15 (2017), 1791-1798

Thybo, P.; Hovgaard, L.; Lindeløv, J.S.; Brask, A.; Andersen S.K. Scaling Up the Spray Drying Process from Pilot to Production Scale Using an Atomized Droplet Size Criterion, Pharmaceutical Research 25-7 (2008), 1610 - 1620

Tolmač, D.; Prvulović, S.; Radovanović, L. Effects of Heat Transfer on Convection Dryer with Pneumatic Transport of Material, FME Transactions 36 - 1 (2008), 45 - 49

Vanslambrouck, B. Heat pumps in drying operations, presentation at NWGD symposium 'Drying: from theory to practice' (2017)

Xia, L.; Gurgenci, H.; Liu, D.; Guan, Z.; Zhou, L.; Wang, P. CFD analysis of pre-cooling water spray system in natural draft dry cooling towers, Applied Thermal Engineering 105 (2016), 1051 - 1060

Yazdanpanah, N.; Langrish, T.A.G. Crystallization and Drying of Milk Powder in a Multiple-Stage Fluidized Bed Dryer, Drying Technology 29:9 (2011), 1046 - 1057

Zbiciński, I.; Li, X. Conditions for Accurate CFD Modeling of Spray-Drying Process, Drying Technology 24:9 (2006), 1109 - 1114

Zbiciński, I.; Piątkowski, M. Spray Drying Tower Experiments, Drying Technology 22:6 (2004), 1325 – 1349